TÉCNICO LISBOA

Assessment and Optimization of Demand Response Technologies in the Smart Grid of Valverde, Évora

Luigi Ghiani

Thesis to obtain the Master of Science Degree in

Energy Engineering and Management

Supervisor: Prof. Carlos Augusto Santos Silva

Examination Committee

Chairperson: Prof. Luís Filipe Moreira Mendes

Supervisor: Prof. Carlos Augusto Santos Silva

Member of the Committee: Prof. Rui Miguel Amaral Lopes

November 2018

InnoEnergy MSc SELECT- Environomical Pathways for Sustainable Energy Systems

Master Thesis in partnership with:

EDP - NEW ENERGY WORLD R&D

Special thanks to the industrial supervisors:

Ricardo Mendes André

Pedro Castro

Abstract

The following document presents a case study analysis of SENSIBLE, a demonstration project implemented in Valverde, Portugal, led by EDP NEW R&D. The main goal is the integration of different storage technologies, photovoltaic energy and a Home Management System (HMS) into a total of 25 households, maximizing the economic benefits for the end customer.

The performance of the project is assessed from August 2017 to July 2018. Then, the HMS is modelled with Matlab to test some demand response strategies, based on day ahead forecasts on the photovoltaic production and the expected electricity demand.

From the analysis, the average Self-Consumption Ratio is 57.23%, and an average Self Sufficiency Ratio is 31.16%. The project generates on average 29 €/month of savings for each customer. From a financial perspective, the most feasible configuration is the installation of a photovoltaic panel with a smart water heater reaches the back in 12 years, with an IRR of 14%.

The model has been tested with different strategies: the application of the new algorithm on the HMS showed potential in shifting the demand to night hours, but does not bring economic benefits.

The carbon footprint of the end customers has been reduced of around 10.9 tonnes of CO_2 equivalent, due to the renewable penetration.

A final discussion on the potential development of such projects across Europe is then introduced, concerning the risk of an unfair redistribution of the grid costs.

Keywords: Demand Response, Smart Grids, Photovoltaic, Forecasts, Energy Storage

Resumo

O seguinte documento apresenta a análise de caso de estudo do SENSIBLE, um projeto de demonstração implementado em Valverde, Portugal, liderado pela EDP NEW R & D. O principal objetivo é a integração de diferentes tecnologias de armazenamento, energia fotovoltaica e um sistema de gestão residencial (em inglês, Home Management System, HMS) num total de 25 residências, maximizando os benefícios económicos para o cliente final.

O desempenho do projeto é avaliado desde agosto de 2017 a julho de 2018. Em seguida, o HMS é modelado com Matlab de forma a testar algumas estratégias de resposta à procura, com base nas previsões do dia seguinte de produção fotovoltaica e a procura esperada de eletricidade.

A partir da análise, o índice médio de autoconsumo é de 57,23%, e o índice médio de auto-suficiência é de 31,16%. O projeto poupa a cada cliente 29 € / mês em média. Do ponto de vista financeiro, a configuração mais viável é a instalação de um painel fotovoltaico com um aquecedor de água inteligente que tem retorno em 12 anos e uma TIR de 14%.

O modelo foi testado com diferentes estratégias: a aplicação do novo algoritmo no HMS mostrou potencial em mudar a demanda para a noite, mas não traz benefícios econômicos.

A pegada de carbono dos clientes finais foi reduzida cerca de 10,9 toneladas de CO_2 equivalente, devido à penetração renovável.

É então apresentada uma discussão final sobre o potencial desenvolvimento de tais projetos em toda a Europa, baseada no risco de uma redistribuição injusta dos custos da rede.

Palavras-chave: Demand Response, Smart Grids, Photovoltaic, Forecasts, Energy Storage

Table of content

Nomenclature

A_{pv}	Area of the photovoltaic panel	[m]
B_c	Battery Capacity	[Wh]
B_{eff}	Usable energy of the battery	[Wh]
B_{max}	Battery maximum charge/discharge power	[W]
$EB_{sensible}$	Electricity bill in SENSIBLE project	[€]
EB_{std}	Electricity bill in the standard case	[€]
$E_{b,in}$	Battery electricity input	[Wh]
$E_{b,out}$	Battery electricity output	[Wh]
E_d	Electricity demand of the appliances	[Wh]
E_{dtot}	Total electricity demand	[Wh]
E_{gen}	Electricity generation	[Wh]
E_{inj}	Electricity injected in the grid	[Wh]
E_p	Electricity purchased from the grid	[Wh]
E_{pv}	Electricity produced by the photovoltaic panel	[Wh]
E_{sc}	Electricity self-consumed	[Wh]
$E_{wh,el}$	Energy consumed by the electric hot water heater	[Wh]
E_{wh}	Electricity consumption of the water heater	[Wh]
GHG_e	Total greenhouse gases emissions	[g $CO_{2\ eq}$]
G_T	Irradiance on the tilted surface	[W]
I_T	Total irradiation on the tilted surface	[Wh]
I_b	Beam Irradiation on the horizontal surface	[Wh]
$I_{d,T}$	Diffuse irradiation on the tilted surface	[Wh]
I_d	Diffuse irradiation on the horizontal surface	[Wh]
I_o	Extra-terrestrial irradiation on a horizontal surface	[Wh]
I_{on}	Extra-terrestrial irradiation on a horizontal surface normal to the beam	[Wh]
P_{pv}	Rated power of the photovoltaic panel	[W]
R_b	Ratio of beam radiation on a tilted surface	
T_{amb}	Ambient temperature	[K]
T_{cell}	Photovoltaic cell temperature	[K]
T_{inlet}	Inlet temperature of the water coming from the pipeline	[K]
T_{max}	Maximum temperature of the water heater	[K]
V_{H2O}	Volume of water	[m^3]
c_{H2O}	Specific heat of water	[J/(gK)]
c_w	Specific heat of water	[J/(gK)]
θ_Z	Zenith angle	[rad]
μ_T	Efficiency of the photovoltaic panel due to temperature	[%]
μ_b	Roundtrip battery efficiency	[%]

μ_{dirt}	Efficiency of the photovoltaic panel due to dirt	[%]
μ_{inv}	Inverter Euro Efficiency	[%]
μ_{module}	Efficiency of the photovoltaic module	[%]
ρ_{H2O}	Density of water	[kg/m^3]
CHP	Combined Heat and Power	
DR	Demand Response	
DSM	Demand Side Management	
HMS	Home Management System	
IEA	International Energy Agency	
PV	Photovoltaic	
SCR	Self-Consumption Ratio	[%]
SSR	Self Sufficiency Ratio	[%]
C	Capacity factor	[%]
CF	Cash Flow	[€/y]
CI	Carbon Intensity	[g $CO_{2\ eq}$]
CPP	Contracted power price	
G	Irradiance	[W]
GHI	Global Horizontal Irradiation	[Wh]
IRR	Internal Rate of Return	[%]
K	Clear Sky Index	[%]
$NOCT$	Normal Operating Cell Temperature	[°C]
NPV	Net Present Value	[€]
$RMSE$	Root Mean Square Error	
i	Interest rate	
m	Air mass	
β	Slope of the photovoltaic panel	[DEG]
ε	Clearness parameter	

List of Figures

List of Tables

1 Introduction

In September 2015, 193 countries signed an agreement named 2030 Agenda for Sustainable Development. The objective of the agreement is to aggregate the efforts of developed and developing countries to achieve worldwide peace and prosperity, end poverty of any kind and, at the same time, protect the planet for the future generations. The success of the project will depend on 17 Sustainable Development Goals (SDGs), macro areas with specific targets to be achieved within 2030. [1] Some of the goals are directly interconnected to the sustainable energy sector, such as: universal access to modern energy by 2030 (SDG 7), urgent action to combat climate change, or dramatic reduction of the emissions of pollutants (SDG 13).

The complete list is presented in Figure 1.

Figure 1: Sustainable Development Goals of the United Nations, pillars of the 2030 Agenda for Sustainable Development. [1]

The specific targets of SDG 7 include an increased share of renewables in the energy mix, a double rate of improvement in energy efficiency, the expansion and upgrade of the infrastructure and of the technologies to provide modern and sustainable energy services.

Regarding the upgrade of the infrastructure, the concept of smart grid is considered one of the key factors [2]. Smart grids connect electricity generation to end users, employing advanced digital technologies to monitor and manage the power flows. The smart grids improve the capability of the system of meeting the various electricity demands and help the grid operators and the market stakeholders to work more integrated and easily. Furthermore, smart grids operate in a more efficient way, reducing the environmental impact and the cost of the

electricity supply chain. At the same time the system reliability, resilience and stability are maximized. Smart grids can be designed and built as new systems, but in most of the OECD countries their implementation needs to be integrated in the current networks, minimizing the impact on the current operation (shortages, power lines interruptions).

1.1 Case study: Euro 2020 Horizon Project SENSIBLE

The development of smart grids in the different countries and regions strongly needs a preliminary test of adequate business models, to fit technology into the local realities. In this context, both small and large-scale pilot projects are necessary. A very interesting case study is given by SENSIBLE, led by Siemens Corporate Technology A.G and NEWR&D/ Labelec, EDP.

SENSIBLE is a demonstration project, with the main goal of integrating different storage technologies, micro-generation and renewable energy into power networks, homes and buildings. The project investigates the possibility to generate value not only for the grid operator, but also for the end customers. SENSIBLE is running in parallel in the following locations:

- Valverde, Évora (Portugal): the village is supplied by a rural grid considered weak, and potentially unreliable. The goal is to integrate thermal and electric storage in the distribution network and in the households, in order to stabilize the voltage at grid level, and to maximise the independence of the single houses from the network;

- Nottingham (United Kingdom): the goal is to foster the environmental commitment of a neighbourhood. The grid doesn't have reliability problems, the focus is more on the market participation of homes and communities to the energy market, integration of storage and energy management technologies;

- Nuremberg (Germany): the implementation happens mainly in the laboratories of THN University. It will focus on the different storage possibilities in buildings, including thermal storage, combined heat and power, electricity and gas.

The project horizon is from January 2015 to December 2018, the budget allocated is 15,4 M€. The participating partners are part of a European Consortium of 13 members, the list is available Annex I: SENSIBLE Project Partners

1.2 SENSIBLE in Valverde, Évora

The main goal of the installations in Évora is to demonstrate the technical and economic feasibility of distributed energy storage and energy management tools in the distribution network, both at grid and household level. Regarding the end customer, the project investigates the opportunity of finding an optimal mix of technologies, suitable for different locations. A good mix of energy generation, storage and management technologies should be able to:

- Increase the distributed renewable penetration and energy independence of the houses;

- Better match the distributed electricity generation and the demand through batteries and thermal storage;

- Show the opportunity for innovative business models, that decrease the electricity bill for the end customer.

It is important to mention that Portugal lacks regulations in terms of participation of the end customers in a flexible electricity market. Hence, an additional goal is to understand the benefits and the impact that new policies, in line with other European countries, might have in smart grids projects in Portugal. Assessing the economic and environmental potential impact of policies is considered key at political level, in the promotion of new regulations. It is expected that a more efficient generation, consumption and retail of electricity, introducing automation and flexibility, can have an impact on the cost of electricity and on the emissions of a country.

In Valverde, a total of 25 customers has been monitored over one year: most of them are residential customers, except for one manufacturing company and a restaurant.

The main components installed in the households of Valverde are a photovoltaic system with related inverter, a smart water heater, a battery and a centralized home management system (HMS) that controls the power flows in the house. Some technical details are presented in Table 1.

Table 1: List of the devices installed in Valverde

	Model: GreenTriplex PM060P00 Version: 260 W module Capacity installed: 1.5 kW Module efficiency: 16.1% NOCT: 46°C Power degradation coefficient: -0.39 % / K Module Area: 1639 x 983 Area installed: 9.3 m^2 Degradation: linear to 80% in 25 years
	Model: Sunny Boy 1.5 Rated power: 1.5 kW AC Max efficiency: 97.2% European Weighted Efficiency: 96.1 %
	Model: LG Chem RESU 3.3 Total Energy: 3.3 kWh Usable Energy: 2.9 kWh Round trip efficiency: 95 %
Picture not available	Water Heater: EnerPlural Maximum power: 2kW (dimmable with PV) Minimum Temperature: 40°C Maximum Temperature: 60°C Capacity: 60 – 200 l

The HMS is currently working with the following prioritization for the electricity produced by the photovoltaic panel:

1. Direct consumption (electric load);
2. Charge of the water heater;
3. Charge of the battery;
4. Injection to the grid.

1.3 Scope of the thesis

The general scope of the thesis is to assess the performance of the equipment installed in SENSIBLE, using data analysis and physical modelling tools to model the households with the hardware and software installed, identify new control strategies, perform a simulation, test the new strategies and compare them with the original HMS algorithm. For more clarity, the scope is broken down in the two main tasks.

1.3.1 Evaluation of the performance

The first task is to assess the performance of the existing home management system in project SENSIBLE for the different households and with the different configurations. The time series of the household consumptions and generation/purchase of the electricity extracted from the data can be used to calculate technical performance indices, and the application of the current tariff schemes provided by EDP allows to analyse the economic and financial sustainability of the project.

1.3.2 Forecast Based Control for Optimization of the HMS

The second task aims to develop a Forecast Based Control of the HMS, based on day ahead forecasts of the solar irradiation and of the electric loads. The optimization tool will be tested on the past year, to allow a comparison with the current system.

The development of the following tools is required:

- Weather forecast algorithm;
- Forecast of the electric load;
- Radiation model and photovoltaic generation;
- DHW consumption generator;
- Model of the HMS.

A literature review is performed to better understand the context and the best way to develop the tools.

Several objective functions are possible, for instance:

- Minimization of the daily expenditure for electricity, calculated on the 24h forecast;
- Maximization of the PV electricity consumption;

The work will focus mostly on the minimization of the electricity bill for the final customer.

2 Literature review

2.1 Smart grids applications

The centralized generation frameworks of the current energy systems are struggling to adapt to the new generation variability and to the demand peaks. The introduction of smart grids allows an easier integration of distributed renewable generation, such as photovoltaic and micro wind, and several other low carbon technologies, such as electric vehicles. Additionally, a more flexible demand would foster the electrification of heating, cooling and industry.

Some of the main characteristics of a smart grid are listed in Table 2.

Table 2: Characteristics of smart grids [2]

Characteristic	Description
Customer information and participation	Customers are informed about their consumption, and they can change their way of purchasing electricity under ad-hoc incentives and offers. In this way, they can contribute in the grid balance (eg. Demand Response).
More generation and storage options	Distributed generation and storage installed by the customers finds better integration in a smart grid.
New products and services	More business models are possible in the controlled environment of the smart grid, allowing for small scale investments for the end users with clear benefits in the medium run.
Improve adequate power quality	Not all the customers require the same power quality. Electricity and consequently price can be differentiated according to the specific need of the different customers.
Equipment efficiency optimization	Dynamic ratings, optimized capacity, maintenance efficiency are some examples of how the equipment can be better controlled if constantly monitored.
More resiliency to problems	The system better reacts to unexpected events isolating the problems while the rest of the network continues with normal operation

Worldwide the interest and consequently the investment in smart grid technologies are growing. The investment growth between 2014 and 2016 accounts for 12% overall. In general, every year more than 10 billion of dollars are invested in the deployment of new technologies in the distribution networks as shown in Figure 2.

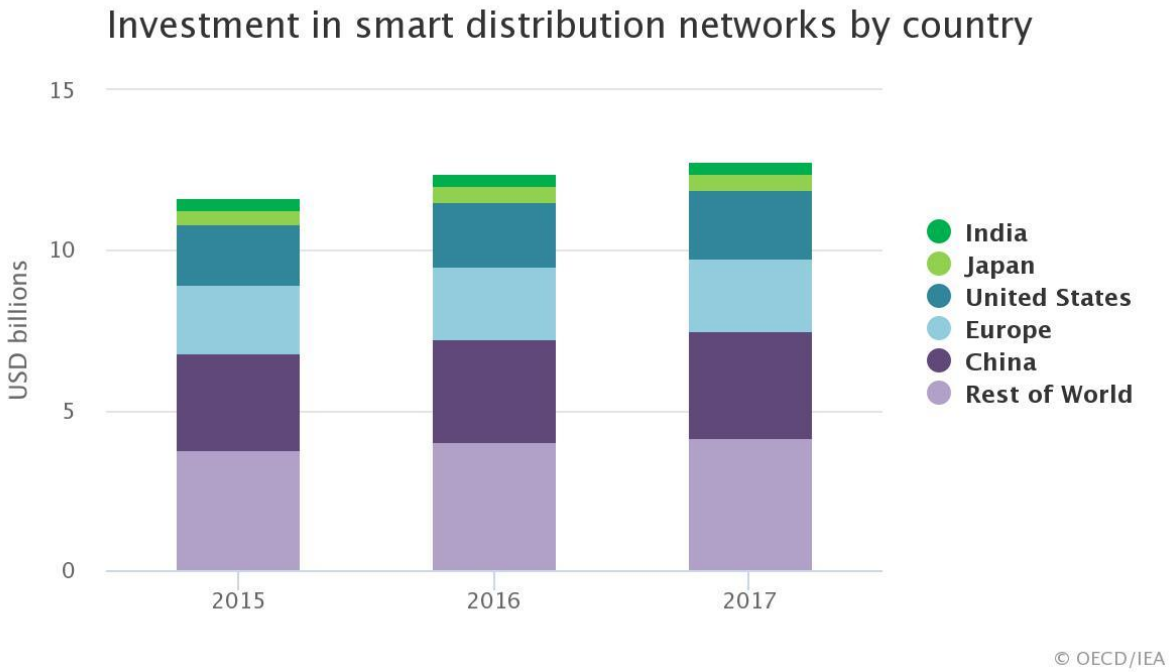

Figure 2: Investment in smart distribution networks by country [3]

The worldwide capillary installation of smart meters is uneven, as shown in Figure 3: China has almost reached full coverage of installation, followed by Japan, Spain and France, which are expected to complete installations in the next years. USA and European Union have reached more than half of the market. Regarding India and Southeast Asia, the development until now has been slower, but it is expected to grow due to a general reduction of the costs, and to the knowledge gained from already existing projects in other countries, that paved the way for profitable investments.

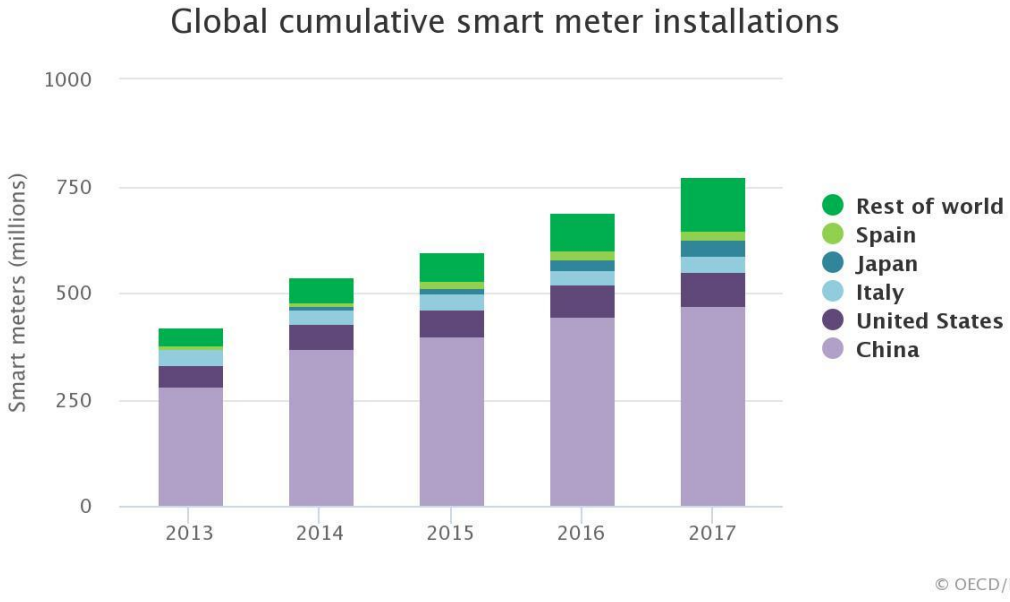

Figure 3: Global cumulative trend of smart meter installations. [3]

2.2 Demand Response

The electricity supply and demand must always be balanced. Historically the grid balance has been achieved mainly by matching the demand in the different hours of the day, adapting the generation. For most of the 20th century, fossil fuels were the main energy source, and their flexibility has been used to supply electricity in a reliable and cheap way. In the first two decades of the 2000, renewables started to be cost competitive, thanks to the incentives of the governments, and in the last years solar and wind generation started to play a major role in the modern energy systems. The cost of new photovoltaic panels has decreased by 70% since 2010, wind by 25% and batteries by 40%. [4]. According to the development scenarios analysed by the IEA (International Energy Agency), by 2040 India and China will have the largest installed capacity of low carbon electricity generation, where the share of renewables is expected to reach 40%. The European Union is going to experience a growth of the installed capacity, and 80% of the new generation will be renewable. In the EU wind is expected to be the main source of electricity after 2030, thanks to the development of both onshore and offshore technologies. The energy transition towards a low carbon future is accelerated by the contribution of households, energy communities, companies investing and benefitting of distributed generation, mainly photovoltaic.

With the introduction of the variable and distributed generation of renewables, and with the rapid increase of their shares in the energy systems worldwide, some integration challenges need to be addressed to efficiently match the electricity supply and demand.

Electricity from renewables is low cost and carbon-free[1], but situations of overproduction happen when there is high availability of natural resources, like strong wind or high solar irradiance, and low demand. On the other hand, when renewable energy availability is low, demand still needs to be met with expensive and carbon-intensive fossil fuel-based generation, such as turbo-gas. These situations are environomically[2] not desirable and show potential for improvements and optimization.

Demand Side Response, or just Demand Response (DSR/DR) is defined as a set of measures where renewables, energy efficiency and electrification interact for the optimal operation of an energy system (refer Figure 4).

[1] Not from a life cycle perspective, but rather from the day by day operation

[2] Environomical: optimal solution from the technical, economic and environmental point of view.

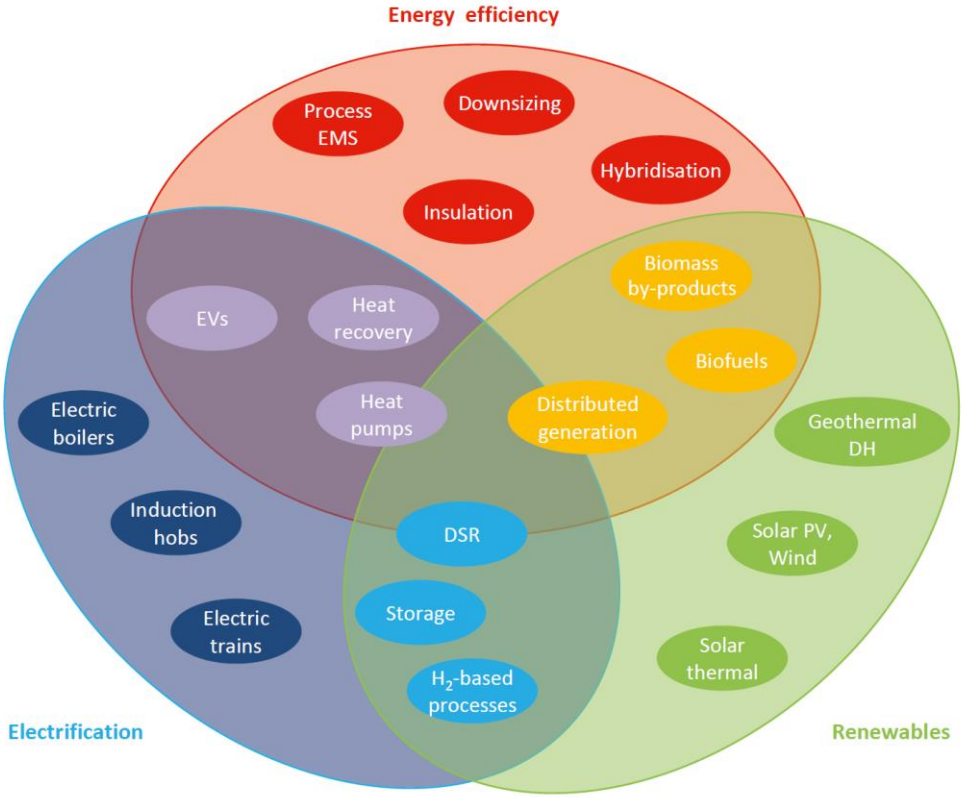

Figure 4: Synergies between Renewables, Energy Efficiency and Electrification [4]

The innovation of DR is to exploit flexibility of the electricity demand to consume energy when naturally available. Consumers are contributing to the grid balance by offering the possibility to adapt part of their demand to the renewable generation. The implementation of DR is a win-win situation: the grid operator more likely avoids supply disruptions or curtailments of renewable generation; the consumers can be paid to change their consumption patterns by shifting or reducing loads, or by offering flexible loads as fast frequency response measure.

The potential for DR applications worldwide is estimated to be around 4,000 TWh per year, which represents about 15% of the total electricity demand. An overview is presented in Figure 5. Flexible loads are mainly found in the commercial and industrial sector, where time dependency of the process can be sometimes relaxed: few examples are represented by large scale heating and cooling, water treatment plants and electric vehicles charge. Flexibility potential can be harnessed also in the residential sector, where a high level of technology for connection and automation is necessary, as well as a figure that can aggregate the customers and optimally manage their flexibility.

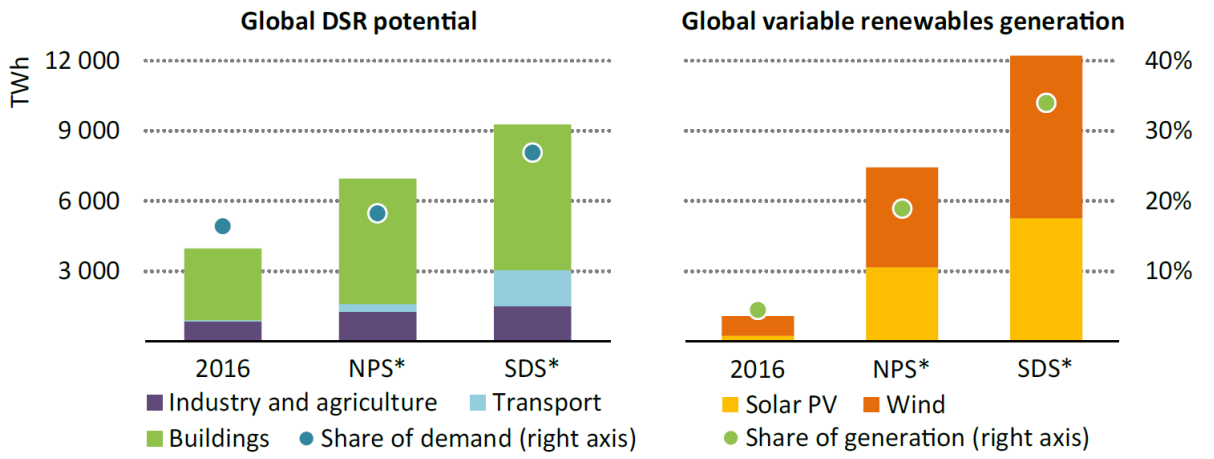

Figure 5: DSR potential and generation from variable renewables in the New Policies and Sustainable Development Scenarios [2]

The application of Demand Side Response requires not only the deployment of technology, but also an adequate policy framework. DSR finds the incentives in the market, where flexibility is priced and remunerated.

2.2.1 Policy Framework and DR Projects in Portugal

There is an indicator that shows the potential application of DR in Portugal: Portuguese customers are very active in the retail electricity market. In fact, during the year 2016, 21% of the Portuguese households changed their electricity retailer, and this percentage is the highest in Europe. Despite this, Portugal is lagging in terms of regulations and market structure. In fact, aggregated demand-side flexibility is not accepted neither in the balancing market nor in the ancillary services. [5] Impeding deregulation on roles and responsibilities, access rights, baselining, measurement, pre-qualification, payment are some of the obstacles for DR spread. Furthermore, Portugal does not have a legal framework for a large-scale implementation of smart metering systems [6].

There is no regulatory framework to define the role of potential DR aggregators, roles and responsibilities and access rights. The Portuguese market presents a very large capacity availability and capped electricity prices, slowing down the DR market development. [7]

One of the legislations available in Portugal that can support the diffusion of DR is represented by the Interruptibility Contracts, available for customers having a contracted power above 4 MW (mostly industrial customers). However, the system operators did not activate such contracts, so interruptible load programs are considered only in emergency cases. With the Ministerial Order N° 41/2017 a new regime of remuneration of the security reserve has been activated, establishing a capacity payment scheme. Electricity market players such as aggregators can guarantee power capacity in critical periods either by providing generation units or by DR programs. Nonetheless, in order to participate to this remuneration scheme, the minimum aggregation threshold is 10 MW.

A first demonstration project is developed by Energy and Industrial Technology Development Organization (NEDO) and the Portuguese National Laboratory for Energy and Geology (LNEG). The project aims at the development of

Automated DR in the Lisbon City Hall and other facilities of the Lisbon Municipality, in particular the automatic control of the variable refrigerant volume of a multi-split air conditioner, with cold air storage. The control system is based on day-ahead weather forecasts and load patterns. The project started in 2016 and will and in December 2019. Other partners are EDP Inovação, Everis and Daikin Industries.

The first peer to peer electricity sharing project in Portugal is represented by NetEffiCity, started in 2016 by Virtual Power Solutions (VPS), with the support of GECAD, a research centre of the Institute of Engineering of the Polytechnic of Porto and of Simples Energia, a Portuguese energy supplier. Held in the three municipalities of Alfândega da Fé, Penela and Vila Real, the goal of the project is the optimization of the purchase of electricity from the market, by considering the distributed generation from photovoltaic panels and the load flexibility of HVAC systems in public buildings.

The company VPS also implemented an Active Energy Management System, a platform called Kisense, in more than 100 banks across Portugal. The system provides energy flexibility services as part of the energy contracts by performing load shedding and load shifting in HVAC systems and optimized aggregated energy management. In 2017 the project led to an average annual energy cost reduction of 17 %, with a potential of increasing this value even more if implemented in combination with Real-Time Pricing.

To sum up, demand response shows potential in Portugal for consumers having considerable thermal flexibility, individual or aggregated. The implementation of pilot scale projects and the very active customers' engagement are considered a key factor to pave the way to the deregulation of the electricity market that will enable DR applications, in particular the Portuguese regulator ERSE should perform a electricity regulatory review to open the market to aggregators in the ancillary services and balancing market.

2.2.2 Finland as Benchmark in DR Application

Finland is currently one of the European countries with the best framework to enable demand response applications [5]. Fingrid, the Transmission System Operator (TSO) allows aggregated loads to enter the reserve market. Fingrid is aware of the importance of DR applications to balance the inflexible generation, considering the high share of renewables in the electricity generation mix (47%) of which the intermittent sources are anyway a small part, with a wind share of 7% and solar less than 1%. [8]

A summary of the markets where DR can be implemented in Finland is presented in Table 3.

Table 3: Markets and DR participations possibilities in Fingrid framework [5]

Market place	Type of contract	Min. bid	DR participation in Jan. 2018
Frequency controlled normal operation reserve (FCR-N)	Yearly and hourly markets	0.1 MW	4 MW
Frequency controlled disturbance reserve (FCR-D)	Yearly and hourly markets	1 MW	430 MW
Automatic frequency restoration reserve (aFRR)	Hourly market	5 MW	0 MW
Balancing power market (mFRR)	Hourly market	5 MW	100 – 300 MW
Balancing capacity market (mFRR)	Weekly auctions	5 MW	

The Finnish Electricity Market is open also for independent aggregators, and DR can be offered to the strategic reserves purchased by the Finnish Energy Authority. With the decree 66/2009, Finnish DSOs were required by law to implement a large-scale smart meter rollout, and currently over 99% of customers in different sectors are equipped with smart metering systems. DSOs are obliged to make hourly consumption data available for the end customers, and online services are available to offer tariffs with more sophisticated DR incentives, suitable for the end users.

2.3 Demand response optimization tools

In the literature, Demand Response optimization is implemented through several different algorithms:

- Genetic Algorithms GA; [5]
- Linear Programming LP; [5]; [6];
- Mixed-integer nonlinear programming; [7];
- Particle Swarm Optimization PSO [8].

There are some modelling tools already available on the market that can be used, two of them are presented in [9]. The study compares the integration of fixed and flexible loads in the dispatch optimization using HOMER®, EnergyPLAN® and a self-built Matlab® model in the case study of the energy system of Corvo Island, Azores. The proposed Matlab® algorithm is a daily economic dispatch model, described more in detail in [5]. The study analyses different strategies to minimize the cost function of the energy system, and in particular, by optimizing the electricity load using a DHW backup. The paper presents a comparison between linear programming and an optimization genetic algorithm.

A genetic algorithm GA is a meta-heuristic optimization approach, that includes stochastic inputs. It is inspired to the natural evolution principles, and incorporates some concepts of genetics like natural selection, crossover, mutation, eletism. The range of application of GA is wide, in engineering, mathematics, biology, it is easy to implement, and it is particularly suitable for constrained optimizations. The algorithm generates a finite population of chromosomes, which are the possible solutions, and exposes them to a fitness function. The chromosomes that achieve the best fit are more likely to be selected as “parents” for the next generation: they are crossed over and mutated, so they generate a new population of “children”, that is expected to have better fit. Repeating this cycle for a certain number of generations, the outcome can be:

- A maximum number of generations is achieved;
- An end-criterion is met, for example, when the fitness of the “offspring” achieved a stable point and does not evolve significantly any more.

The paper concludes that GA is a useful methodology to approach DR dispatch and scheduling with an adequate number of populations, also thanks to its versatility. The same authors have used GA in other case studies, for instance in [10], where a solar thermal system is coupled with demand response for domestic hot water DHW, in isolated microgrids where share of renewable electricity generation is more than 25%. The optimization shows positive impact on the final emissions compared to fossil fuel-based water heaters (up to 88%).

2.3.1 HOMER® Pro

HOMER® Pro, developed by HOMER Energy, is a recognized and well-known software for modelling the integration of renewables into grid-connected and off-grid energy systems. It performs an economic optimization, minimizing the Net Present Cost (NPC) of the system and consequently the levelized cost of electricity (LCOE). The

optimization engine has been originally developed by the National Renewable Energy Lab (NREL). Several academic studies are performed with this software: [11] presents a list of hybrid renewable energy systems analysis, where HOMER® is the most used tool. The software is also used in [12] and [13]. Furthermore, there are papers where HOMER® is used for DR modelling: in [14] HOMER® is combined with another tool in an isolated grid, [15] investigates DR in a water treatment plant, in [16] renewable penetration is fostered using DR on a Gasification plant.

HOMER® allows to define a certain percentage of the total load that is deferrable, specifically the input parameters are the average daily deferrable load for each month and the maximum peak load. This option is not very flexible, and the way HOMER® elaborates DR presents some drawbacks, for instance:

- Flexible loads have a lower priority, and they are met only in off-peak hours or in presence of RE generation excess;
- It is not possible to input the hours at which the flexible loads would normally be met;
- HOMER® considers only the electricity demand and does not include the thermal energy demand.

For these reasons, HOMER® Pro is not the appropriate tool for the scope of this work.

2.3.2 HOMER® Grid

HOMER® Grid is a new software developed by HOMER Energy in 2018, and more specific it is suitable for behind-the-meter applications. The software is particularly useful for distributed generation systems and it works with the same optimization engine of HOMER Pro. The interface of the two tools is very similar but, in this case, it presents a more detailed tab for the photovoltaic panel, for the tariff modelling and introduces the input of thermal loads. The software seems particularly useful to simulate household energy dynamics and includes options for load shifting and peak shaving. However, is not considered useful for the proposed work for two main reasons:

- It is not possible to include thermal loads met only by electric heaters, the natural gas boiler is always requested to start a simulation;
- Even though there is an interface for the battery, the hot water tank is not implemented, and therefore there is no possibility to model a thermal storage.

2.3.3 EnergyPLAN®

EnergyPLAN® is a software to simulate large scale energy systems, for instance energy flows at national level. It includes electricity, heating, cooling, industry and transport sector. The simulations are performed on an hourly basis. The software is available for free and it has been developed by the Sustainable Energy Planning Research Group, from the Danish Aalborg University.

EnergyPLAN® is not suitable for this specific phase of SENSIBLE, which requires the control of the single house's system. Nevertheless, it might be useful to consider it EnergyPLAN® to understand the impact of SENSIBLE or similar projects at regional level in the future. For instance, it would be interesting to draw scenarios of the impact of increased solar energy share in Alentejo.

2.4 Weather forecast methodologies

Renewable generation potential is dependent on weather conditions. Forecasting solar irradiation or wind speed is extremely important when planning the dispatch of generators and storage in an energy system with

considerable penetration of renewables. Short-term forecasts at intra-hour level are necessary for a more effective operation, grid balancing and for real-time unit dispatching. Forecasts for a longer time horizon, for example day ahead, are useful to schedule storage and loads to shift, very important when controlling a microgrid with thermal or electric storage.

Several methodologies are assessed and summarized in [17]. In [18] the impact of renewables' forecasts is analysed in the optimization of demand response technologies of a microgrid system in Corvo Island in Azores, Portugal. In the paper, hot water tanks are studied as storage and as electric loads that can be shifted. Short-term forecasting methods are used to build a day-ahead schedule, and the Clear Sky Persistence Model is selected due to its simplicity. The model is described in detail in [19], and it is based on the knowledge of the clear sky irradiance, that is the solar irradiance with no clouds and with good sky conditions of radiation transmittance. The assumption of the model is that the clear sky index of a certain time step persists for the following one.

Eq. $$K(t+\Delta t) = K(t) = \frac{GHI_{measured}(t)}{G_{clr}(t)} \quad (1)$$

Eq. $$GHI_{forecast}(t+\Delta t) = K(t) G_{clr}(t+\Delta t) \quad (2)$$

Where:

- $K(t)$ is the clear sky index at the time step t;
- $GHI_{measured}(t)$ is the GHI measured at ground level;
- $GHI_{clr}(t)$ is the GHI for clear sky conditions.

The paper proposes a variation of the model using the clearness index instead of the clear sky one. The difference is the use of the extra-terrestrial Solar Irradiance GHI_o, defined as the solar irradiance outside the atmosphere. The clearness index is hence defined as:

Eq. $$k(t+\Delta t) = k(t) = \frac{GHI_{measured}(t)}{GHI_o(t)} \quad (3)$$

And consequently, the equation (2) can be written as:

Eq. $$GHI_{forecast}(t+\Delta t) = k(t) GHI_o(t+\Delta t) \quad (4)$$

It must be noticed that the persistence model is more accurate for locations with typical stable weather conditions.

A different forecast method is presented in [20], called the Solar Forecast Similarity Method. It predicts the following day irradiance and irradiation using a statistical method from the long-term study of HelioClim-3

database[3]. The solar irradiation dataset is available at the SoDa Solar Radiation Data website[4], that offers several datasets and services related to solar irradiation worldwide, connected with MINES ParisTech University.

The Similarity Method searches in the database the most similar days to the current one, and extracts for each of them the following day. These following days are then averaged hour by hour to obtain a forecast. To detect the similar days, the criteria is the minimum of the square distance for each day, given by the difference for each hour of the day. Considering the database value x, the reference day i and the corresponding value y:

$$Eq. \qquad d_i^2 = \sum_h (x_h - y_{ih})^2 = \sum_h (x_h^2 - 2x_h y_{ih} + y_{ih}^2) \qquad (5)$$

The quality of the forecast is determined by several parameters:

- The length of the time horizon of the database y;
- The number of similar days considered when analysing the current day;
- The weight given to different years when looking for similar days

Like the persistency method, the effectiveness of the similarity method depends on the climatic characteristics of the area analysed. Areas with very stable conditions are easier to forecast than fast-changing regions.

2.5 Electric load modelling

A model of the household electricity demand with high time resolution is challenging to develop and represent a critical factor for DSOs. In fact, having a reliable model for the electric load would allow to make forecasts, useful to guarantee the stability of the system and to efficiently dispatch generation and storage.

The domestic load curve is specific for each house and differs in magnitude and shape according to a wide range of parameters, for instance:

- Number of people living in the house;
- Consumption habits;
- Breakdown of the appliances.

In the case study of SENSIBLE, due to data protection and privacy regulations most of these details are unknown and have to be considered implicit in the data.

In the literature several models are proposed: electricity use can be investigated via bottom-up approach, starting from data or assumptions made on the activity of the household, appliances and their use, occupancy. Aggregating details on the consumption patterns allow the generation of a typical load curve for the household. The most cited

[3] HelioClim-3 is a satellite-derived solar radiation database. It exploits the Heliosat-2 method to estimates a "cloud index", based on the analysis of the 15 minutes Meteosat Second Generation (MSG) satellite images in the visible band. More information available at http://www.soda-pro.com/soda-products/hc3-archives

[4] SoDa has been developed by O.I.E. (Observation, Impacts, Energy). This is a common laboratory (or structure) of MINES ParisTech and ARMINES. More information available at http://www.soda-pro.com/about-us/actors

examples of bottom-up approaches are analysed in [21] and in [22]: in general they need a relevant amount of data and assumptions and tend to be very complex.

When it comes to making predictions, the most challenging factor to consider is represented by the consumption habits, behavioural variables that are very specific for the household. [23] proposes a high-resolution stochastic model of multiple electricity-dependent activities in households, based on a Markov-chain to describe the consumption habits. The model identifies a list of activities, for instance cooking or using specific appliances, and then generates a sequence of activity state transitions in every discrete time step. A transition probability $p_{ij}(k)$ from state i to j is defined as:

$$p_{ij}(k) = \frac{n_{ij}(k)}{n_i(k)} \quad \textit{Eq.} \quad (6)$$

Where:

- $n_{ij}(k)$ is the total number of transitions between state i and j;
- $n_i(k)$ is the total number of transitions from state i.

Another possible approach is the top-down, starting from the aggregate load curve directly without having detail on the specific information required by the household, but just the aggregate consumption. Both the bottom-up and top-down models can be either deterministic or stochastic: the second ones can be based on Markov chains or probability distribution functions. [24] presents a bottom-up electric load modelling methodology with probability distributions fit. The distributions are tuned using a high-resolution electricity use dataset from Swedish households. The paper makes a literature review of the best distributions to model electric loads and selects the Weibull and Log-Normal distributions, since they don't consider negative values of power consumption, unlike the Normal distribution. The equations of the distributions used to code the model have been included in Annex III: Distributions for Electric Load Forecast

The advantage of this model is that it allows to transform real use data into a stochastic model, that can create realistic time series using Monte Carlo simulations. However, a considerable amount of data is necessary, preferably with sub-hourly time resolution. Furthermore, two important assumptions are made:

- For each timestep, the demand of the household is a random outcome and so completely independent;
- The probabilities for all the possible load levels can be considered continuous functions.

In the paper the data are clustered according to some relevance criteria to consider seasonal and type of day variabilities. The scheme proposed is to create separate distributions for:

- Each hour of the day;
- Each day of the week;
- Each month of the year.

2.6 Radiation models for photovoltaic generation

The estimation of the photovoltaic electricity production requires technical information on the selected panel, and a physical model for the solar radiation. In fact, most databases present time series of measurement of the Global Horizontal Irradiance (GHI) and Direct Normal Irradiance (DNI). The electricity generated by the panel can be estimated from the following information:

- Technical details of the panel and inverter, available from the datasheet of the manufacturer: module efficiency, inverter efficiency and power losses due to temperature;
- Solar radiation and temperature historical data;
- A solar radiation model to calculate the radiation on the tilted surface;
- Some additional correction factors, like a dirtiness coefficient.

The main reference for the physical model is [25], so all the presented equations can be found in this book. The Perez Radiation model has been selected for this work, being one of the most accurate models available. The Perez Model coded in Matlab is validated through the following steps:

- Simulation of the tilted radiation using the solar data of Valverde;
- Estimation of the generation and of the efficiency of the panel due to temperature;
- Comparison with the average photovoltaic generation from data.

The Perez model represents the projection of the GHI into a tilted surface of slope β. In general, all the radiation models are approximations necessary to quantify the diffuse radiation that reaches a panel. This model is conservative, and it slightly underestimates the diffuse radiation. The model is more accurate in the central hours of the day then in the early morning or late afternoon, when the diffuse radiation plays a key role. A summary of the radiation components is graphically shown in Figure 6.

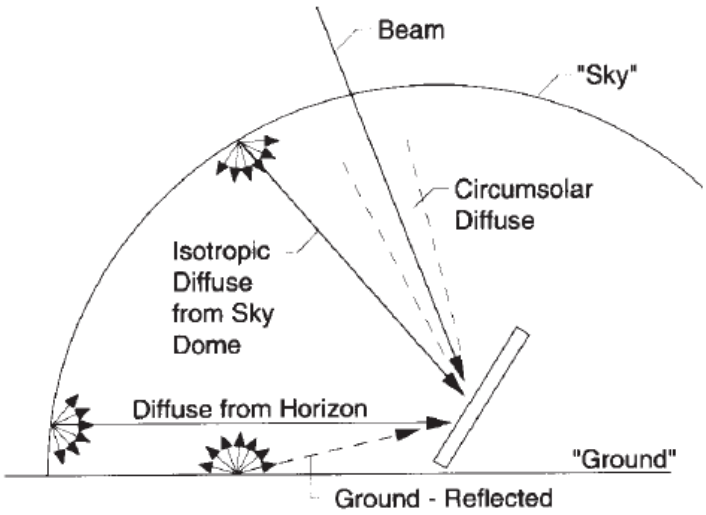

Figure 6: Components of the radiation on a tilted surface [26]

The Perez model is considered the best model available with regards to the way the diffuse radiation is considered, and its component of the circumsolar diffuse and horizon brightening. The complete model is defined in the equation:

$$I_T = I_b R_b + I_d(1 - F_1)\left(\frac{1 + \cos\beta}{2}\right) + I_d F_1 \frac{a}{b} + I_d F_2 \sin\beta + I\rho_g\left(\frac{1 - cos\beta}{2}\right) \quad \textit{Eq.} \quad (7)$$

The equation is composed of five terms: the beam, the isotropic diffuse, the circumsolar diffuse, the diffuse from the horizon, and the ground-reflected radiations. The projection of the direct component is given by the first term: the ratio of beam radiation on a tilted surface to that of a horizontal surface given the incidence angle θ is:

Eq. $$R_b = \frac{\cos\theta}{\cos\theta_Z} \quad (8)$$

The three diffuse components of the radiation are summarized in the equation of the total diffuse radiation on the tilted surface:

Eq. $$I_{d,T} = I_d\left[(1-F_1)\left(\frac{1+\cos\beta}{2}\right) + F_1\frac{a}{b} + I_d F_2 \sin\beta\right] \quad (9)$$

Where:

- F_1 and F_2 are the circumsolar and horizon brightness coefficients;
- Coefficients a and b depend on the angles of incidence of the cone of circumsolar radiation on the tilted and horizontal surface.

The coefficients a and b can be calculated as:

Eq. $$a = \max(0, \cos\theta), \quad b = \max(\cos 85\,, \cos\theta_Z) \quad (10)$$

The components of the diffuse radiation are treated in the following way:

- The fraction of circumsolar diffuse radiation as it is coming from the beam direction;
- The remaining part of the diffuse radiation as perfectly isotropic;
- A term of horizon brightening radiation.

Three parameters need to be defined. The clearness is function of the diffuse radiation and of the normal incidence beam radiation:

Eq. $$\varepsilon = \frac{\frac{I_d + I_{b,n}}{I_d} + 5.535\ \cdot 10^{-6}\theta_Z^3}{1 + 5.535\ \cdot 10^{-6}\theta_Z^3} \quad (11)$$

The brightness parameter is:

Eq. $$\Delta = m\ \frac{I_d}{I_{on}} \quad (12)$$

Where m is the air mass, and I_{on} is the extra-terrestrial irradiation on a horizontal surface normal to the beam. The extra-terrestrial irradiation estimated as:

Eq. $$I_{on} = 1367\ (1{,}00011 + 0{,}034221\cos B + 0{,}00128\sin B + 0{,}000719\cos 2B + 0{,}000077\sin 2B); \quad (13)$$

The air mass for zenith angles from 0° to 70° can be estimated with the equation:

Eq. $$m = \frac{1}{\cos\theta_z} \quad (14)$$

For higher zenith angles, to take into account the effect of the Earth curvature the air mass can be calculated as:

Eq.
$$m = \frac{\exp(-0.0001184\, h)}{\cos(\theta_z) + 0.} \quad (15)$$

The result can be projected to obtain the extra-terrestrial irradiation on a horizontal surface, given the zenith angle θ_Z:

Eq.
$$I_o = I_{on} \cos\theta_Z \quad (16)$$

The brightness coefficients F1 and F2 are functions of statistically derived coefficients for ranges of values of ε:

Eq.
$$F_1 = \max\left[0, \left(f_{11} + f_{12}\Delta + \frac{\pi\theta_Z}{180} f_{13}\right)\right] \quad (17)$$

Eq.
$$F_2 = \left(f_{21} + f_{22}\Delta + \frac{\pi\theta_Z}{180} f_{23}\right) \quad (18)$$

The brightness coefficients can be extracted from Table 4

Table 4: Brightness coefficients for Perez Anisotropic Sky [26]

Range of ε	f_{11}	f_{12}	f_{13}	f_{21}	f_{22}	f_{23}
1.000–1.065	−0.008	0.588	−0.062	−0.060	0.072	−0.022
1.065–1.230	0.130	0.683	−0.151	−0.019	0.066	−0.029
1.230–1.500	0.330	0.487	−0.221	0.055	−0.064	−0.026
1.500–1.950	0.568	0.187	−0.295	0.109	−0.152	−0.014
1.950–2.800	0.873	−0.392	−0.362	0.226	−0.462	0.001
2.800–4.500	1.132	−1.237	−0.412	0.288	−0.823	0.056
4.500–6.200	1.060	−1.600	−0.359	0.264	−1.127	0.131
6.200–∞	0.678	−0.327	−0.250	0.156	−1.377	0.251

More information on the calculation of the solar angles are available in Annex V: Solar angles

.

2.7 Domestic Hot Water

Domestic Hot Water DHW heating for households can be centralized or individual. Centralized systems are typical of Nordic countries, where Combined Heat and Power CHP cycles use low-temperature heat for the district heating. Distributed DHW systems can be solar based, electric or fuel powered.

Electric water heating in Portugal accounts for more than 5% of the annual residential electricity demand [27]. Like the electric load, DHW usage depends on behavioral factors (activities performed, amount of water used for each activity) and on the structure of the household, like the number of people living in the house. However, compared to electricity, thermal energy can be stored more easily and in a cheaper way, enabling a partial dissociation between the time when the water is heated up and the time when it is consumed. In a variable price tariff scheme for electricity, this dissociation gives room for demand response applications.

In [28], a good classification of the types of electric loads is presented, concerning the possibility of the application of DR strategies:

Table 5: Load control types proposed by [28]

Control type	Description	Appliances
Uncontrollable loads	Loads that can't be controlled without decreasing the quality of the energy service	Lighting, office and entertainment equipment, cooking appliances and others
Re-parameterizable loads	Loads that can be controlled thermostatically, with possibility of reset the parameters	Cold appliances, air conditioning systems, electric water heaters
Interruptible loads	Loads that can be completely interrupted for short periods without affecting the end user	Cold appliances, air conditioning systems, electric water heaters
Shiftable loads	Loads that can be delayed or anticipated with respect to the end user preference	Washing machines, clothes dryers, dishwashers, electric water heaters

According to the definitions proposed by Table 5, electric water heaters have a considerable flexibility in terms of control, because they can be re-parameterizable, interruptible and shiftable. The different control strategies can also be applied simultaneously.

From [10] the equation that describes the electricity converted into thermal energy and stored in the water heater is:

Eq.

$$E_{wh,el} = \frac{V_{H2O} \cdot \rho_{H2O} \cdot c_{H2O} \, (T_{max} - T_{inlet})}{3600} \, [Wh_{el}] \tag{19}$$

Where V_{H20} is the DHW demand, in liters.

3 Data quality analysis and preliminary information

The work is based on real data from the dataset provided by EDP. Before starting the performance analyses, the dataset has been checked and treated to improve the accuracy of the results, and consequently to derive meaningful models.

3.1 Data description and availability

The outcome of the work is strictly connected to the proper understanding and analysis of the dataset provided for the 25 customers of Valverde. The main objective of the data analysis in this work is to extract useful information to understand the dynamics and the performance of the equipment installed from August 2017 to July 2018. The timestep of data recording is 15 minutes, for a total of 96 measurements per day. The parameters available for each customer in each timestep are the following:

- Battery input;
- Battery output;
- Grid purchase: electricity from the network;
- Grid injection: electricity sold to the network;
- Photovoltaic generation;
- Water Heater input: electricity stored in the smart water heater;
- Battery state of charge SOC;
- Water heater temperature.

The mentioned categories can be distinguished in off peak and peak period, according to the bi-hourly tariff scheme. A screenshot of the original dataset file is available in Figure 7.

Timestamp	Date	Hour	'OffPeak_BatteryEnergy'	'OffPeak_BatteryEnergyAMinus'	'OffPeak_EBEnergy'	'OffPeak_EBEnergyAMinus'	'OffPeak_PVEnergy'	'OffPeak_WHEnergy'	'Peak_BatteryEnergy'
13/02/2018 05:45	13/02/2018	05:45:00	0	0	204	0	0	1	
13/02/2018 06:00	13/02/2018	06:00:00	0	0	198	0	0	1	
13/02/2018 06:15	13/02/2018	06:15:00	0	0	220	0	0	1	
13/02/2018 06:30	13/02/2018	06:30:00	0	0	201	0	0	1	
13/02/2018 06:45	13/02/2018	06:45:00	0	0	199	0	0	1	
13/02/2018 07:00	13/02/2018	07:00:00	0	0	209	0	0	1	
13/02/2018 07:15	13/02/2018	07:15:00	0	0	208	0	0	1	
13/02/2018 07:30	13/02/2018	07:30:00	0	0	475	0	0	256	
13/02/2018 07:45	13/02/2018	07:45:00	0	0	368	0	2	172	
13/02/2018 08:00	13/02/2018	08:00:00	0	0	245	0	8	24	

Figure 7: Screenshot of the original dataset [29]

The customers can be divided in different categories, according to the type of equipment installed. All the 25 customers have installed the photovoltaic panels, 10 customers only have the smart water heater, 9 of them only have the battery and 6 of them have both (refer Figure 8).

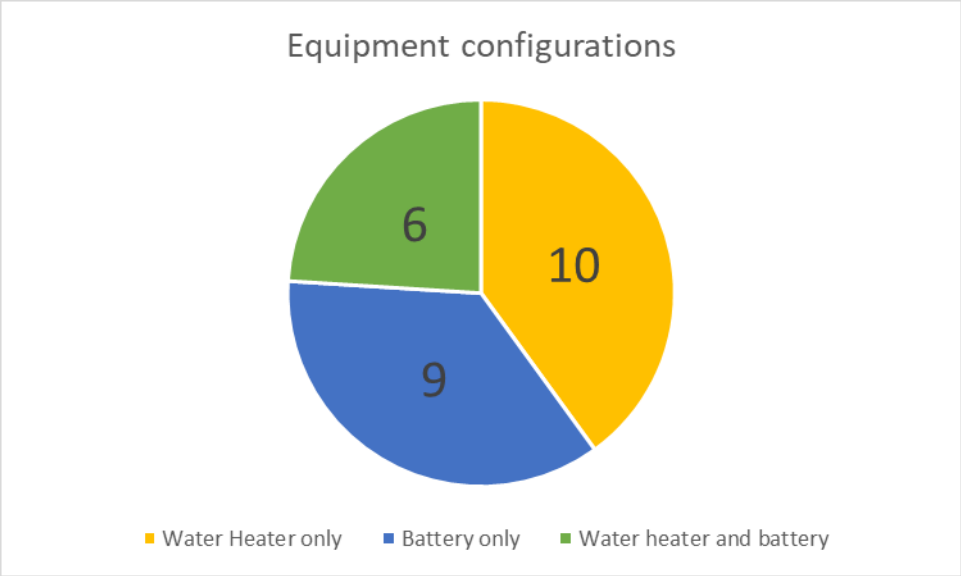

Figure 8: Configurations of the installed equipment

Most of data are available since 27th July 2017. However, during the first week the dataset presents several issues, such as repeated numbers, long series of zeros and missing values, probably due to the initial set up of the data acquisition. The chosen reference day to start the analysis from is the 5th of August 2017. Some other data are available only from 9th of September. In general, not all the customers have been metered for the same number of days, due to different periods or missing days: a summary is available in Figure 9.

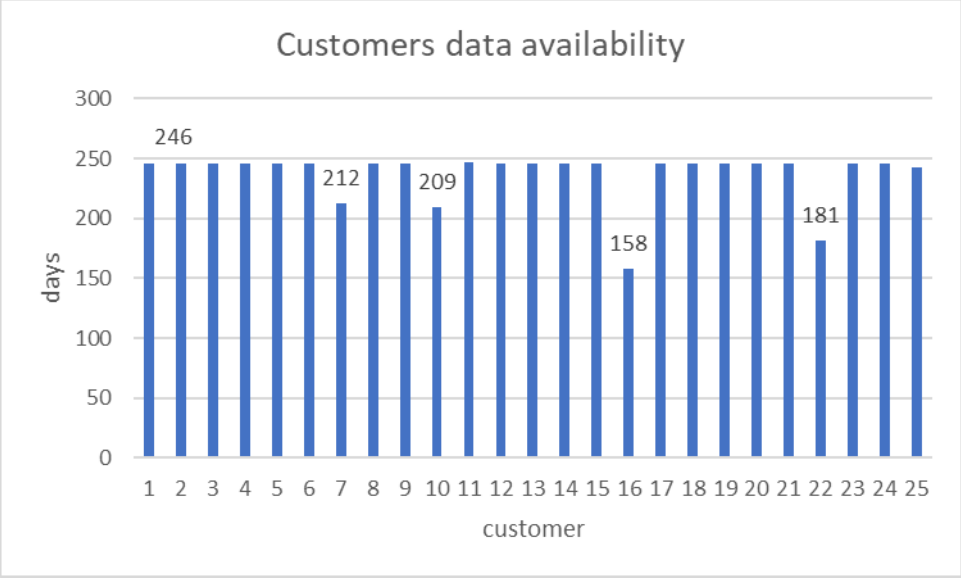

Figure 9: Number of days of metering for each customer, overview

The data already has been preliminary treated before the beginning of this work. Hence, some values are missing in the tables and the data result partially fragmented. To estimate the magnitude of this first intervention, the effective data availability has been estimated for each of the variables under analysis as:

Eq.

$$Availability = \frac{N° \ of \ data}{Maximum \ possible \ data} = \frac{N° \ of \ data}{days \ \cdot 96} \qquad (20)$$

A complete and accurate analysis cannot be performed for all the customers. For instance, customer 20 has a very limited availability of data regarding grid purchase and injection (< 50%), consequently the quality of its analysis is considered poor of significance.

3.2 Problems of the dataset

The dataset presents some frequent issues that might affect the quality of the work. For instance:

- Not all the customers have the same starting and finishing date, as mentioned above;
- The dataset sometimes misses entire days, or even longer periods
- Sometimes the data are apparently available, but all the values are zero (mostly with data of batteries);
- There are situations where the data acquisition system gets stuck and returns the same number for several days in a row.

Regarding long periods of missing data, some of them are due to different starting point of measurements, while others are just due to errors in the acquisition. A summary is presented in Table 6.

Table 6: Missing days from the dataset

customer	Missing from	to	days
C7	09/08/2017	08/09/2017	30
C16	09/08/2017	27/09/2017	49
C10	6/03/2018	22/04/2018	47
C16	05/03/2018	08/04/2018	34
C18	24/05/2018	17/06/2018	24
C22	09/08/2017	29/09/2017	51
C22	29/03/2018	15/04/2018	17
C24	09/02/2018	18/02/2018	9
C25	27/06/2018	09/07/2018	13

3.3 Data filters

To improve the quality of the data used, some filters have been applied to eliminate inconsistencies or clear misfunctions in the data acquisitions. As previously mentioned, the acquisition system sometimes replicates the same value for several time slots, probably due to lag in the communication. This situation is very frequent, an example can be seen in Figure 10.

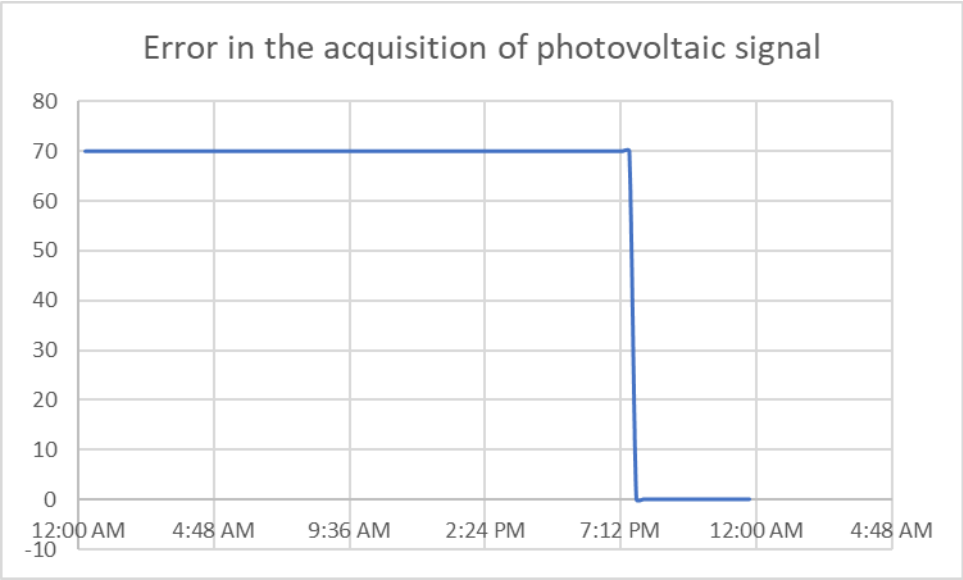

Figure 10: Abnormal photovoltaic signal, example from customer 2, 22 November 2017

Furthermore, it has been noticed that the system sometimes returns in one single timeslot the sum of many previous ones. The result is a value that is inconsistent in the context, like shown in the example of Figure 11. In fact, the maximum discharge power of the battery is 3 kW, resulting in 750 Wh in a timeslot of 15 minutes, while here we have more than 3000 Wh in 15 minutes, totalling 12 kW.

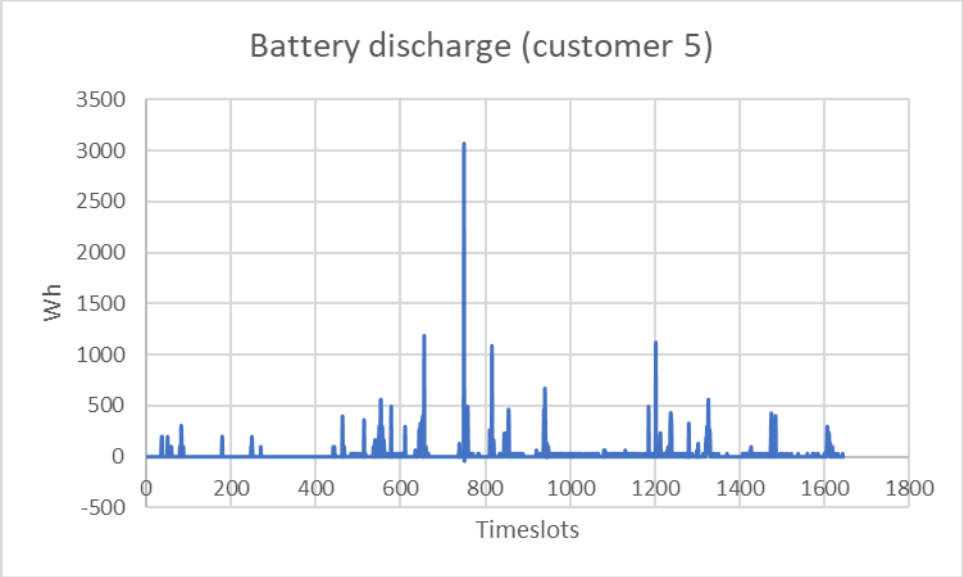

Figure 11: Abnormal value of the energy from battery discharge, shown in a context of 17 days. 15/11/2017 19:15

The main filters applied are expected to identify:

- Photovoltaic generation higher than zero recorded during the night;
- Repeated values;
- Abnormally high values, not consistent with the timeslot.

The filtered values have been erased from the dataset and, when possible, replaced according to specific data repair criteria. In particular for the sake of this work, photovoltaic data are the only ones considered repairable, due to the fact that all the customers have installed the same panel with the same configuration (size, orientation and tilt). The remaining data have not been repaired.

3.3.1 Errors in night data photovoltaic acquisition

The data regarding photovoltaic electricity production are considered of primary importance: a first step in the quality screening is to check the consistency of the production during daytime. A filter has been specifically realized to check photovoltaic production recorded for mistake during night hours.

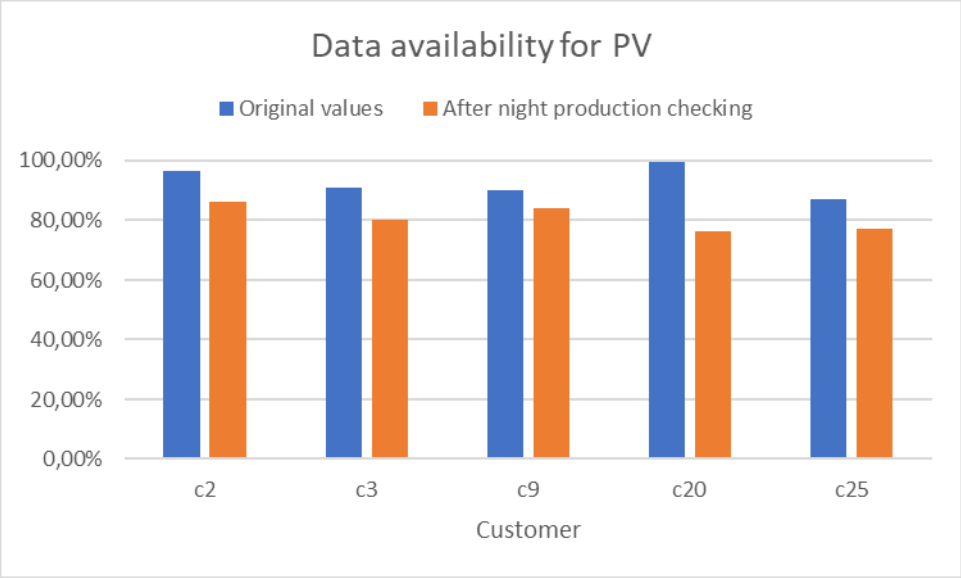

Figure 12: Impact of the data filter used to check consistency of photovoltaic generation, screening night production

In Figure 12 a summary of the most affected customers in the database is presented: for customer 20 for example, more than 23% of the data has been erased.

3.3.2 Repeated values

The filter looks for values repeated in long sequences and erases them. This filter applies to all the variables except the battery input and output. In fact, it must be noticed that the power delivered by the battery is very discretized, in particular in the initial months of aquisition, hence the values are repeated very often, and the filter might erase significant records. An overview of the impact of the first two filters can be seen in Figure 13.

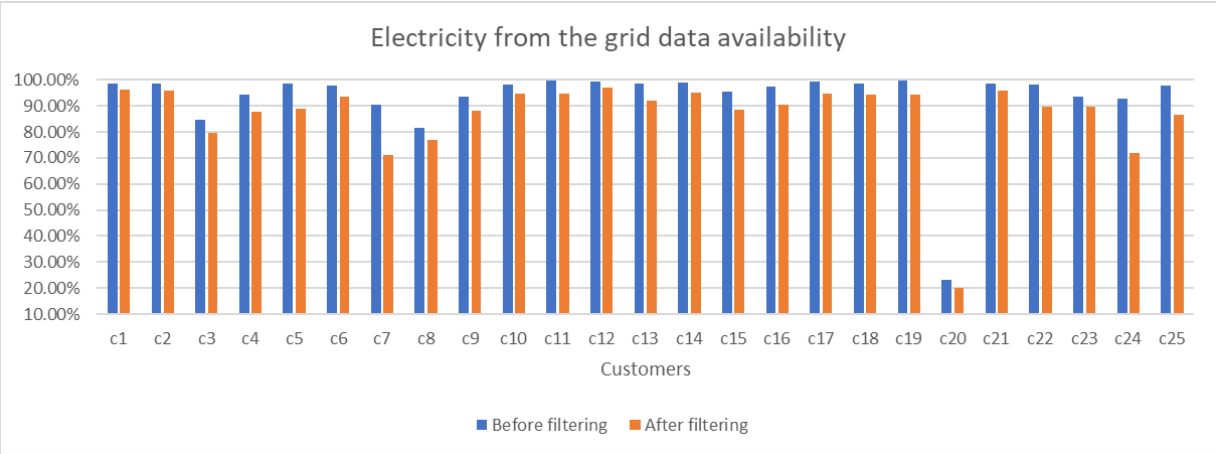

Figure 13: Availability of data of the electricity purchased from the grid

From this graph an important issue emerges for customer 20: the data availability for the electricity purchased from the grid is very low, this has a strong negative impact on the reliability of the results for this customer.

Most of the data missing from the dataset can not be repaired, because they are dependent on the individual habits of the households. The only parameter that can be compared and hence fixed is the photovoltaic electricity production, due to the similar configuration of the photovoltaic installation.

3.4 Photovoltaic data restore

After the application of the filters, data poor of meaning have been erased. In some customers, the fragmentation can increase up to 40%. To increase the accuracy of the analysis, the dataset can be partially restored.

The photovoltaic panels have all the same rated power of 1.5 kW, and they are all installed due south. It is reasonable to use data from complete datasets to fill the gaps in fragmented customers due to the following facts:

- Same equipment is installed, with the same configuration;
- The customers are in the same location and consequently same irradiance conditions;

Still some differences appear among customers, probably due to shadowing and reflection conditions, and other random parameters that cannot be specifically identified. To maximise the accuracy, the monthly electricity generation from the panel has been compared among the customers using the Root Mean Square Error RMSE:

Eq.

$$RMSE = \sqrt{\frac{\sum(E_{pv,x} - E_{pv,ref})^2}{12}} \tag{21}$$

Where:

- $E_{pv,x}$ is the monthly electricity photovoltaic production of the customer object of the comparison;
- $E_{pv,ref}$ is the monthly electricity photovoltaic production of the reference customer, of which the dataset requires repair;

A schematic example can be seen in Figure 14.

Hour	Pv Customer x	Pv Customer y
8:00	80	-
9:00	90	93
10:00	100	102

Figure 14: Example of filling missing data with customers with complete dataset

Some data cannot be replaced because they are missing in all the customers. The goal of the repair of photovoltaic production data was set to reach at least 95% of the availability for each customer, and it has been successfully reached with the proposed method. The result obtained can be seen in Figure 15.

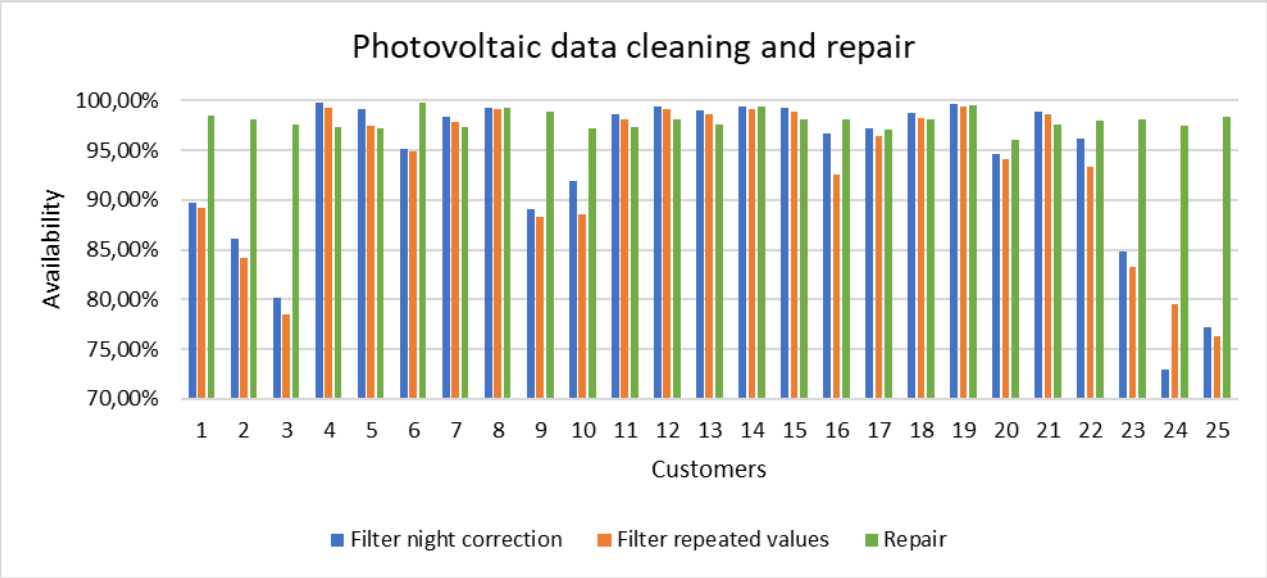

Figure 15: Impact of photovoltaic data manipulation on the data availability

4 Methodology

In this chapter the methodology used for the analysis is presented. The main equations used in the dataset are shown, as well as how the main variables, like the electric load, are derived from computations on the data.

4.1 Main equations

The main equation of the electric load derives from a combination of most of the parameters measured, and in particular three types of energy demand are identified:

- Thermal demand, or electricity stored in the water heater E_{wh};
- Total Electricity Demand of the customers, including thermal consumption E_{dtot};
- Electricity Demand excluding the water heater E_d, that means electric load of the appliances;

The equation that describes the total electricity demand is:

$$Eq. \quad E_{dtot}(t) = B_o(t) - B_i(t) + E_p(t) - E_{inj}(t) + E_{pv}(t) = \Delta B(t) + \Delta E_g(t) + E_{pv}(t) \quad (22)$$

Where:

- ΔB is the balance of the battery, defined as Battery Output minus Battery Input $B_o - B_i$;
- ΔE_g is the balance of the grid, defined as Grid Purchase minus Injection $E_p - E_{inj}$;
- E_{pv} is the electricity produced by the photovoltaic panel;

The electricity demand excluding the domestic hot water takes into account all the other appliances, such as lighting, cooking, fridge, and it is obtained by subtracting to the previous equation the water heater demand:

$$Eq. \quad E_d(t) = \Delta E_b(t) + \Delta E_g(t) + E_{pv}(t) - E_{wh}(t) \quad (23)$$

A scheme representing the previous balance is presented in Figure 16. The equation 22 and 23 generate secondary variables, after all the filters applied to the data and presented in paragraph 3.3.

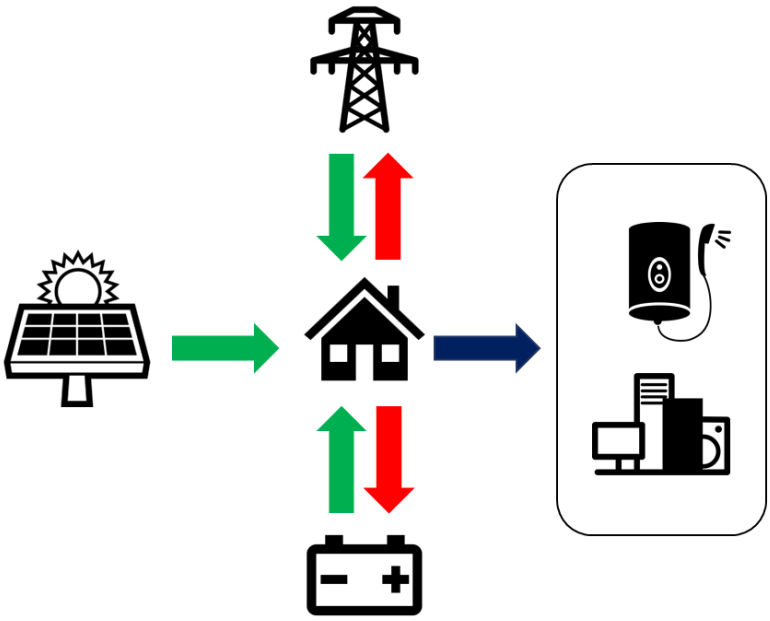

Figure 16: Summary of the connections of the household

4.2 Customers Analysis

4.2.1 Photovoltaic generation

As previously mentioned, all the customers have the same model of photovoltaic panel, installed facing south. A similar electricity generation for all the customers is expected from the analysis. After the repair process mentioned in section 3.4, some values are still missing, due to the different starting point of the data record. In fact, customer 7 is missing one month, while customer 16 and 22 are missing two months (refer 3.2). A summary is presented in Figure 17.

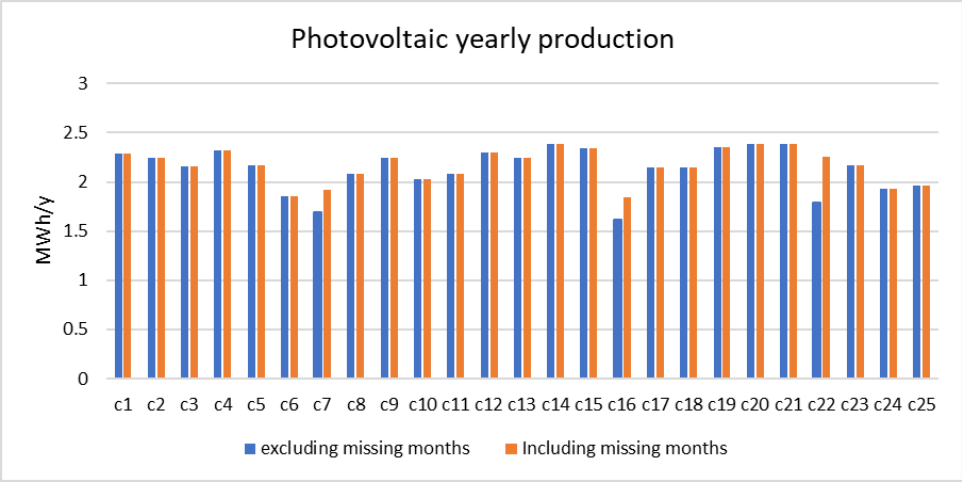

Figure 17: Photovoltaic generation of the customers, including the months missing from the dataset

The average photovoltaic production is 2.17 MWh/y, with a minimum of 1.84 MWh/y for customer 16 and a maximum of 2.38 MWh/year for customer 21. Considering the average photovoltaic production as reference, the minimum and the maximum value differ of 25%: differences of cleanliness of the panel, shading and reflection can

be responsible for this deviation. Also, the data availability and repair might have affected the quality of the information of the dataset.

The capacity factor of each customer can be calculated as:

$$Eq. \qquad C = \frac{E_y[\frac{kWh}{y}]}{P_{pv} \cdot 8760} \qquad (24)$$

Where P_{pv} is the rated power, E_y is the yearly electricity production and 8760 is the number of hours in a year. The results for all the customers are presented in Figure 18.

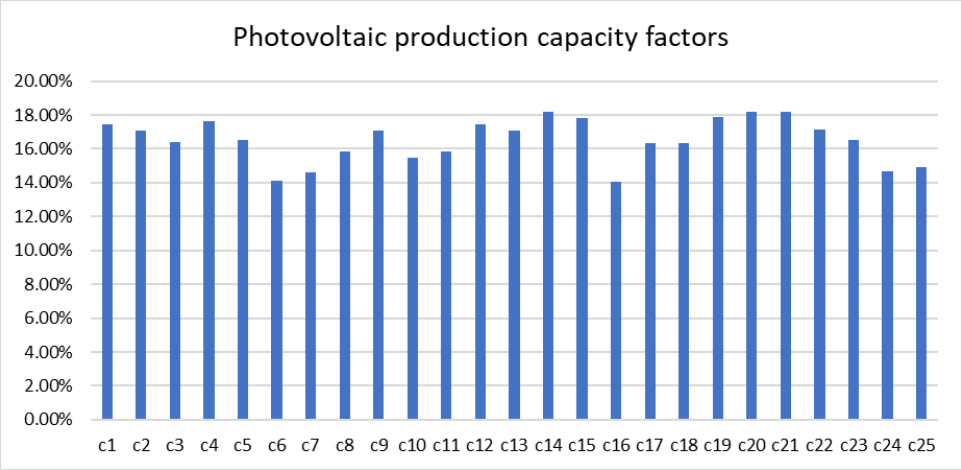

Figure 18: Capacity factor of the photovoltaic electricity production in one year

The average capacity factor is 16.51%, with a minimum of 14.04% for customer 16 and a maximum of 18.17% for customer 14.

4.2.2 Electricity consumption

The electricity consumption has been estimated according to equation 22. A summary of the yearly consumption can be seen in Figure 19, and the customers can be classified as follows:

- 13 customers below 5 MWh/y of consumption;
- 10 customers between 5 MWh/y and 10 MWh/y;
- 2 customers above 10 MWh/year.

The customers missing one or two months have been completed by using the average consumption, in orange in the Figure 19. This completion has been performed only for the sake of the cumulative consumption calculation and does not appear in the time series used to calculate secondary data.

Customer 10 and 18 have a very high consumption profile compared to the other ones: customer 10 corresponds to the manufacturing company and customer 18 to the restaurant. Customer 10 totals 26.91 MWh/y being the largest electricity consumer. Customer 8 has the smallest electricity consumption, with 1.5 MWh/y.

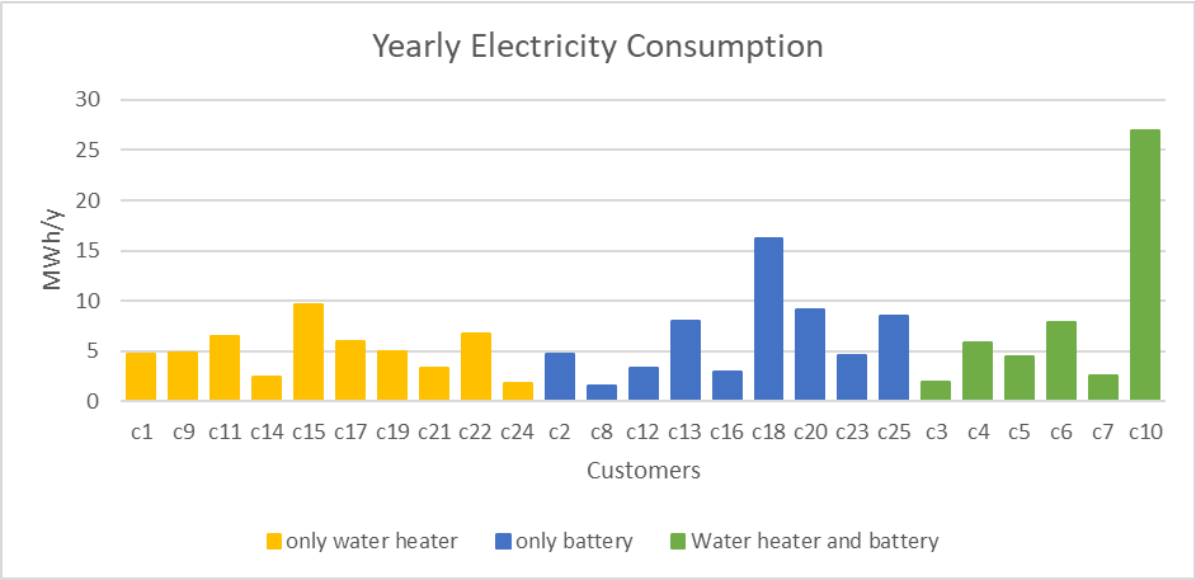

Figure 19: Yearly electricity consumption of the customers of Valverde

The average electricity consumption per capita in Portugal is 4.85 MWh/y [30], in Valverde the average is 5.06 MWh/y if only the residential customers are considered, and 6.38 MWh/y if also the restaurant and the manufacturing company are included. It is important to remember that the values calculated include both the electricity consumed for the appliances and the thermal consumption of the water heater, when applicable. The two components are evaluated and shown separately only for the customers having significant availability of data (> 75%) regarding the water heater electricity input. The values are presented in Figure 20.

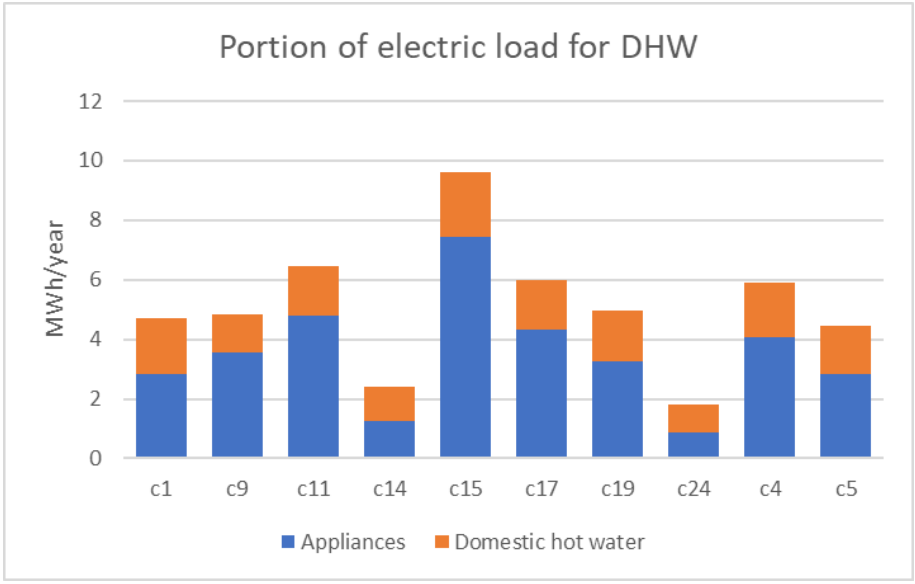

Figure 20: Portions of electricity consumption for the appliances and the domestic hot water

4.2.3 Domestic Hot water consumption

The smart water heater has been installed in 15 households. Each customer has a different capacity of the water heater, an overview is presented in Table 7. Due to the high data fragmentation, 5 customers can't be analysed in terms of thermal consumption.

Table 7: Size of the water heater installed in each household

customer	Size [l]	Data availability
C1	200	Yes
C3	160	No
C4	160	Yes
C5	200	Yes
C6	200	No
C9	120	No
C10	200	No
C11	160	Yes
C14	90	Yes
C15	120	Yes
C17	120	Yes
C19	120	Yes
C21	120	No
C22	60	Yes
C24	120	Yes

The average consumption is 1.46 MWh/y, with a maximum of 2.18 MWh/y for customer 15 and a minimum of 0.94 MWh/y for customer 24. This difference is considered possible due to the different habits, number of people in the house and to some missing data. An overview is presented in Figure 21.

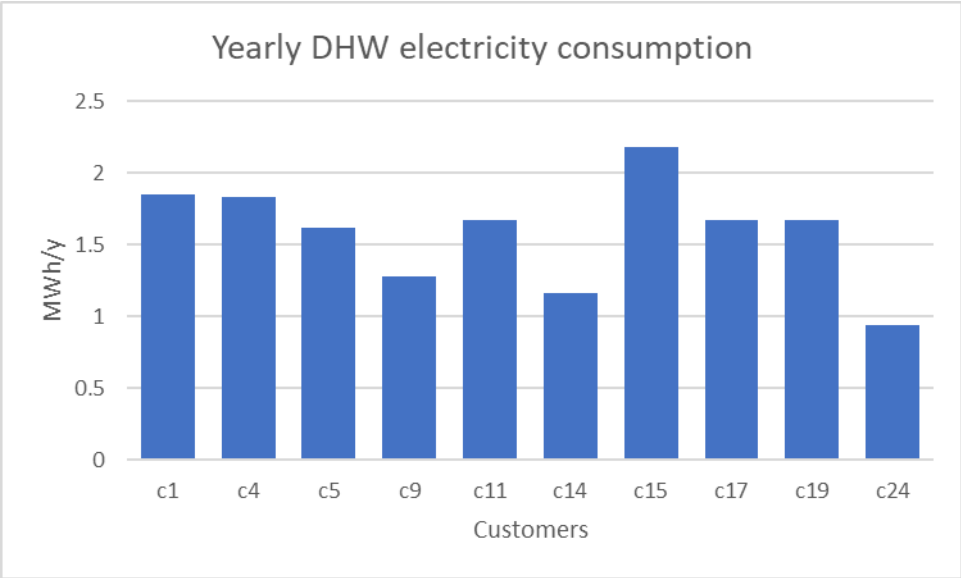

Figure 21: Electricity consumed for the domestic hot water heater in one year

The average share of the electricity consumption related to the hot water heater is 34%. The results are shown in Figure 22.

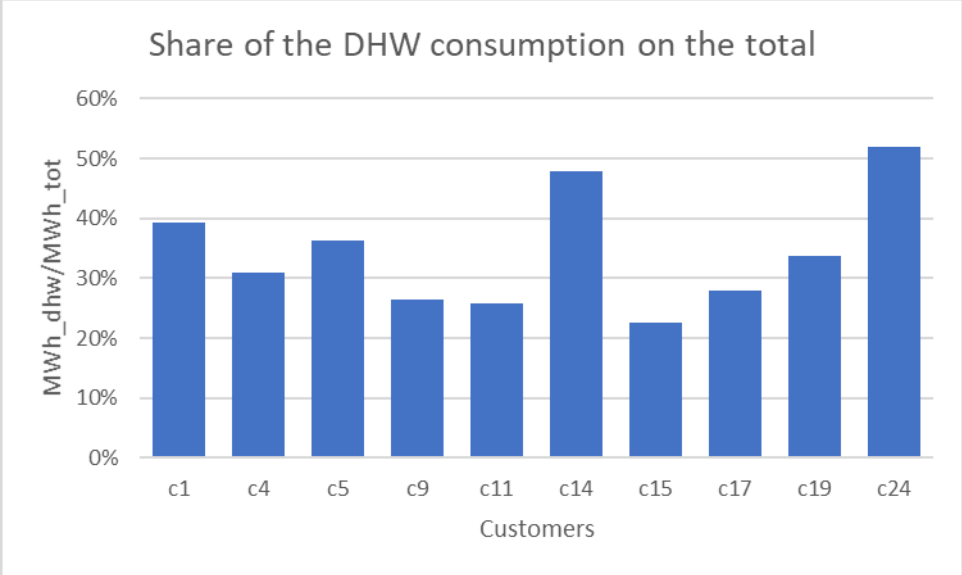

Figure 22: Share of the thermal load in the total electricity consumption

The electricity consumption due to the domestic hot water is very variable with the period of the year. This trend can be seen in Figure 23, where all the customers have been represented. The customers that have a drop in one specific month are probably missing some data from that specific period.

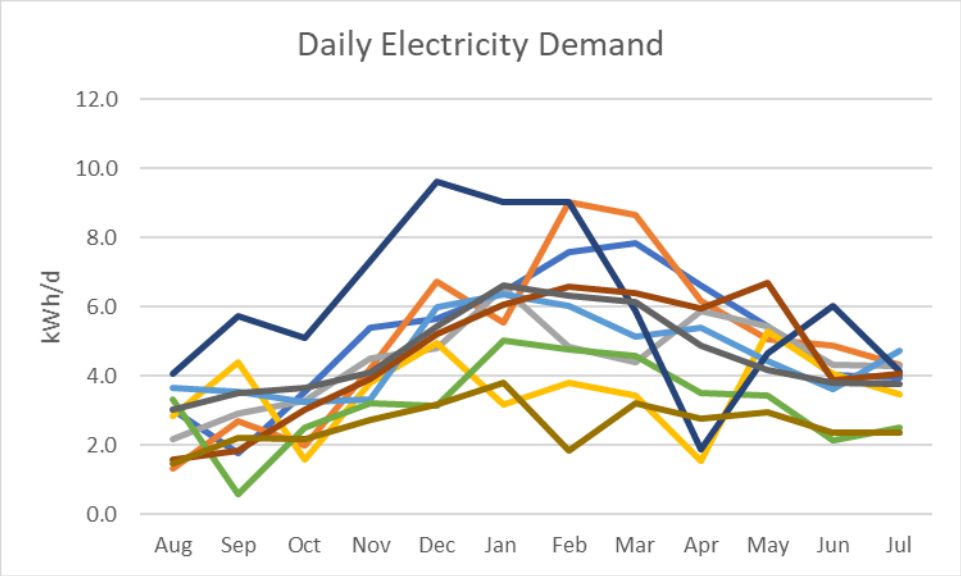

Figure 23: Daily average electricity demand for the water heater

4.3 Technical and Economic Performance Parameters

4.3.1 Self-Consumption and Self-Sufficiency Ratio

The literature suggests several parameters to describe the technical performance of photovoltaic distributed generation in matching the demand [31]. The way the electricity is consumed depends on the instantaneous availability of solar energy and the instantaneous electricity demand. For instance, there could be overproduction production when there is no demand and the opposite: both cases would lead to a poor performance of the system.

The electricity self-consumed can be calculated as:

$$E_{sc}(t) = E_{pv}(t) - E_{inj}(t) \quad \text{Eq. (25)}$$

Where:

- $E_{pv}(t)$ is the electricity produced by the photovoltaic panel;
- $E_{inj}(t)$ is the electricity injected to the grid, in this case study coming only from the excess photovoltaic generation and never from the battery.

Two parameters mainly can be identified: the first one is the Self-Consumption Ratio (SCR), defined as the ratio between the electricity self-consumed in every timeslot and the total photovoltaic production. It is a measure of how much the renewable electricity produced is effectively consumed within the system. In other words, it is a measure of how the system is efficient in not injecting into the grid:

$$SCR = \frac{\sum_{j=1}^{n} E_{SC,j}}{\sum_{j=1}^{n} E_{pv}} \quad \text{Eq. (26)}$$

The second parameter is the Self-Sufficiency Ratio. This parameter has the same numerator, but it is referred to the total electricity demand of the household, so it is a measure of how much of the electricity need is met by the self-consumed energy. In other words, it is a measure of how the system is efficient in not purchasing from the grid:

$$Eq. \quad SSR = \frac{\sum_{j=1}^{n} E_{SC,j}}{\sum_{j=1}^{n} E_{dtot,j}} \quad (27)$$

The two parameters are described in [32].

4.3.2 Savings on the Electricity Bill

To calculate the savings on the electricity bill, the same tariff scheme has been applied to all the customers. Tariffs are available on the webpage of "EDP Tarifarios" [33] and a screenshot of one of the tariffs has been included in Figure 24. No feed-in tariff has been considered for the sake of this work.

The tariffs applied by EDP can be of three types:

- Simple (flat tariff);
- Bi-hourly, with peak tariff applied from 9:00 AM – 10:00 PM and off peak the rest of the time;
- Tri-hourly.

The customers of Valverde have a Bi-hourly tariff scheme, with a contracted power of 6.9 kW peak. The tariff applies the following:

- Price for the contracted power: 0.3835 €/day;
- Off-peak price: 0.0969 €/kWh;
- Peak price: 0.2028 €/kWh.

Eletricidade		Preço EDP
Potência (€/dia)		0.3835
Energia (€/kWh)	Fora de Vazio	0.2028
	Vazio	0.0969

Figure 24: EDP Bi-hour tariff scheme

The cost of electricity can be calculated for the base case where SENSIBLE equipment is not installed, and for the case study of the project. To calculate the electricity bill for each customer in the base case (std), the following equation is applied:

$$Eq. \quad EB_{std} = n \cdot CPP + \sum_{i=1}^{x} 0.0969 \cdot E_{dtot,i} + \sum_{j=1}^{y} 0.2028 \cdot E_{dtot,j} \quad (28)$$

Where:

- CPP is the contracted power price [€/d];
- $E_{tot,i}$ is the electricity demand in off-peak hours;

- $E_{dtot,j}$ is the electricity demand in peak hours;

The bill coming from the currently installed configuration can be calculated with a similar equation, that considers only the electricity purchased from the grid available from the timeseries:

$$Eq. \quad EB_{std} = n \cdot CPP + \sum_{i=1}^{x} 0.0969 \cdot E_{p,i} + \sum_{j=1}^{y} 0.2028 \cdot E_{p,j} \quad (29)$$

In absolute terms, the savings are referred to the standard bill the customers would pay without project SENSIBLE, so paying all the electricity needed for the demand.

$$Eq. \quad EB_s = EB_{std} - EB_{sensible} \quad (30)$$

In relative terms, the savings can be expressed as:

$$Eq. \quad EB_{s,r} = \frac{EB_{std} - EB_{sensible}}{EB_{std}} \quad (31)$$

Where:

- EB_s are the savings on the electricity bill;
- EB_{std} is the standard bill the customer would have without SENSIBLE;
- $EB_{sensible}$ is the actual bill after SENSIBLE project.

4.4 Matlab Simulation Model

To implement a new energy management algorithm for the house, firstly it is necessary to reproduce the behaviour of the current HMS implemented in SENSIBLE. A model has been implemented in MATLAB©, using customer 5 as reference. Some parameters need to be shaped according to a specific household, but potentially they can be set specifically for each customer. The criterion of choice for this case is that customer 5 has both hot water heater and battery, the data availability is high, and the overall performance is good.

The model replicates the current prioritization of the excess electricity, considering technical constraints and efficiencies of the various components, for instance the maximum power that the battery can deliver or absorb (3 kW), or the maximum power of the electric resistance of the water heater (2 kW).

4.4.1 Global Horizontal Irradiation day-ahead forecast

To forecast the photovoltaic potential for the day ahead, the Similarity Model described in section 2.4 can be applied to the time series of irradiance data for the year 2018. Satellite based data of the hourly irradiance of Valverde have been found in Copernicus Atmosphere Monitoring Service (CAMS)[5]. It must be noticed that usually satellite-based radiation data do not have a high level of accuracy, compared to ground measured ones. However, ground measured data were not available for this work.

The Similarity Model has been implemented in MATLAB©, tested using a 15-minutes based database from 01/01/2008 to 31/07/2017, and validated using the year of observation of the project, from 05/08/2017 to 31/07/2018. For each day, considering a timestep of 15 minutes, the RMSE has been calculated as:

Eq.

$$RMSE = \sqrt{\frac{\sum(GHI_f - GHI_e)^2}{96}} \tag{32}$$

The results obtained are shown in Figure 25: The average RMSE is 15.5 Wh/m2, which can be considered an overall satisfactory result.

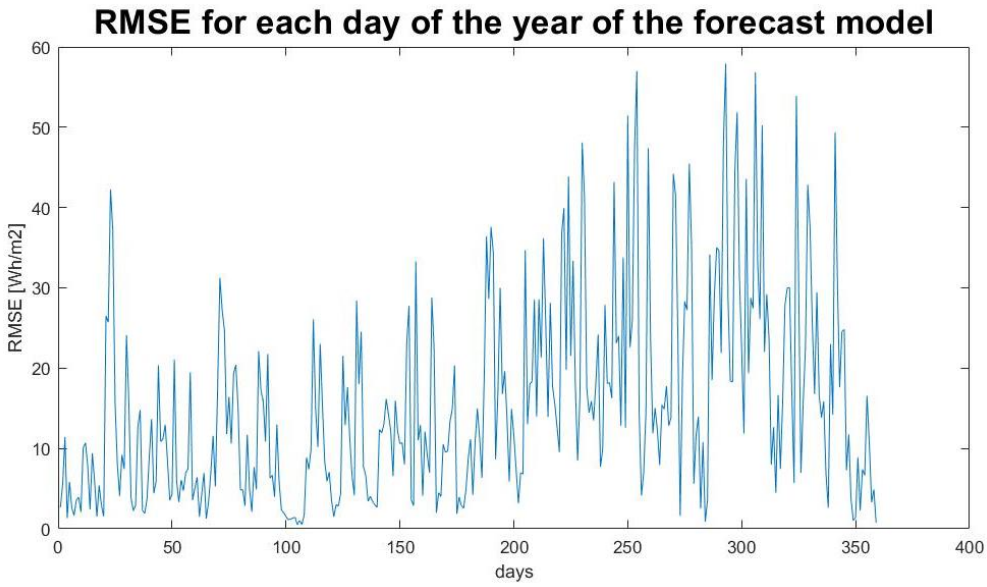

Figure 25: RMSE of the weather forecasts

For completeness, the worst and the best forecasts are presented in Figure 26 and Figure 27.As expected, clear sky estimates are really good, while in cloudy days the estimate are poorer. In the figures, the label “real day” is referred to the satellite measurement coming from Copernico database.

[5] http://www.soda-pro.com/web-services/radiation/cams-radiation-service

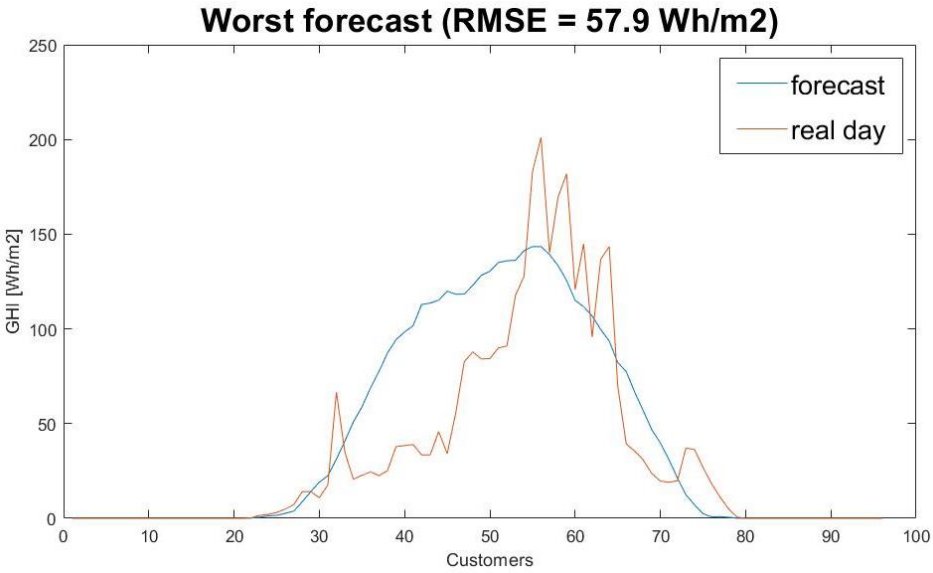

Figure 26: Worst forecast of the Similarity Model

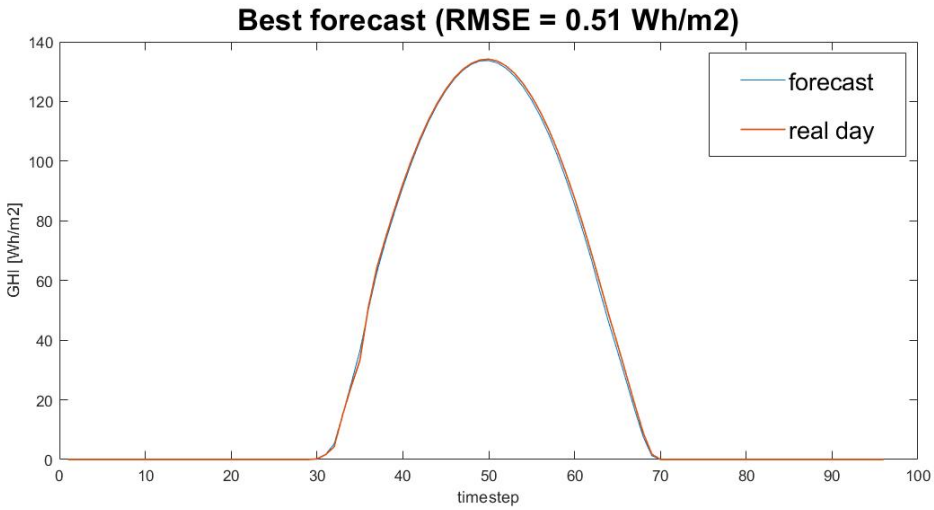

Figure 27: Best forecast of the similarity model

4.4.2 Photovoltaic generation

To calculate the photovoltaic electricity production, some parameters can be extracted from the technical details of the manufacturers, others can be calculated from the literature.

Eq.
$$E_{pv} = I_T \cdot A_{pv} \cdot \mu_{module} \cdot \mu_T \cdot \mu_{dirt} \cdot \mu_{inv} \quad (33)$$

The parameters are presented in Table 8.

Table 8: Parameters for the calculation of the photovoltaic electricity

symbol	Name	Value - Formula
I_T	Total radiation on the panel	Perez model
A_{pv}	Area of the panel	9.3 m^2
μ_{module}	Module efficiency	16.1 %
NOCT	Normal Operating Cell Temperature	46 °C
μ_T	Efficiency due to temperature	-0.39% / K
μ_{dirt}	Correction factor due to dirt	98%
μ_{inv}	Inverter Euro Efficiency	96.1%

The cell temperature is necessary to estimate the temperature derating coefficient. The equation to estimate the cell temperature is:

$$T_{cell} = T_{amb} + \left(\frac{NOCT - 20}{0.8}\right) G_T \quad (34)$$

Where G is the irradiance on the tilted surface, that can be derived from the irradiation of 15 minutes as:

$$G_T = \frac{I_{15m}}{0.25} \quad (35)$$

The ambient temperature has been taken from the MERRA-2 database from NASA[6]. [34]

4.4.3 Domestic hot water model

The hot water heater works with variable ranges of temperature, that can be set by the customers. In the model presented, the water heater operates between 45°C and 53°C. When the temperature goes below 45°C, the electric resistance heats up the water with a power of 2kW until the temperature reaches around 48°C. When charged with solar energy the power is dimmable, and the temperature can go up to 53°C.

The energy balance of the water heater is determined by equation:

$$E_{wh,net} = V_{H2O} \cdot \rho_{H2O} \cdot c_{H2O} \, (T_{max} - T_{inlet}) \text{ [J]} \quad (36)$$

Where:

- V_{H2O} is the volume of water heated up;

[6] https://gmao.gsfc.nasa.gov/reanalysis/MERRA-2/

- ρ_{H2O} is the water density, that can be assumed 1000 $\frac{kg}{m^3}$ at ambient conditions of temperature and pressure;
- c_{H2O} is the specific heat of water, 4186 $\frac{J}{kg\ K}$
- T_{max} is the maximum temperature inside the water heater, assumed 60 °C;
- T_{inlet} is the temperature of the water coming from the pipelines. Generally, it is between 15-20°C, assumed 17.5°C.

With the mentioned assumptions, the electric storage capacity of the water heaters can be calculated as:

$$E_{wh,el} = \frac{V_{H2O} \cdot \rho_{H2O} \cdot c_{H2O}\ (T_{max} - T_{inlet})}{3600}\ [Wh_{el}] \quad \textit{Eq.}\ (37)$$

The results for the customers under analysis are available in Table 9. The conversion efficiency through joule effect is considered 100%, the thermal losses of the water heater are calculated in a further moment.

Table 9: Thermal and electrical capacities of the water heaters, considering a minimum temperature of 40 °C.

customer	capacity	Maximum storable energy [Wh $_{th}$]
c1	200	8721
c4	160	6977
c5	200	8721
c11	160	6977
c14	90	3924
c15	120	5233
c17	120	5233
c19	120	5233
c22	60	2965.1
c24	120	5930.2

The hot water is consumed throughout the day, mostly during the hours where the occupants are awake. The reload of the water tank occur when the photovoltaic panel produces electricity or when the temperature of the water heater goes below 45°C.

Even though the real capacity of the water heater of customer 5 is 200 litres, the amount of energy consumed by the water heater never corresponds to the equation of the energy balance. The reason is that many phenomena occur during the replacement of water and the temperature measurement:

- The probe is placed close to the outlet pipeline, so it measures only one part of the tank;

- Stratification occurs in the water tank, so the temperature profile is distributed along the height of the tank. This temperature difference can be very significant;
- When water is consumed, the reload of cold water leads to a water mixing, before the heating up process starts.

For the water heater analysed to create the model, three situations have been observed:

- Heat up process due to thermal losses, when temperature goes below 45°C;
- Heat up process when the water is consumed due to a considerable water consumption (eg. a shower), and mixing occurs;
- Temperature reduction after a shower is taken.

To simplify the description, a significant water consumption will be mentioned as "shower". For each of the mentioned processes, an equivalent capacity has been identified to match electricity input and temperature measurements. This equivalent capacity has been empirically identified by observing the temperature profile variations and the correspondent electricity consumption. Average values have been selected to create a simple model of the processes happening in the water heater.

- Thermal Losses: 0.5°C/15 min, static warm up process from 44°C to 50 °C, 100 Wh, 12.5 kg of water involved;
- Photovoltaic static warm up process, from 45°C to 53°C, 45 litres of water involved;
- Thermal load: every shower involves 45 litres of water, with a temperature loss of the water heater of 28 °C on average, 1.454 kWh of thermal energy
- Charge after a shower: it involves the same energy of the thermal load, plus the energy needed to restore the temperature at 45°C.

To model the hot water demand, two main aspects were considered:

- The number of showers per day and the distribution in time of this event;
- The amount of water used for each shower.

To make the model more realistic in terms of the number of showers per day and when they occur, the temperature data of the water heater have been analysed and the event shower has been counted as the number of times the water heater temperature goes below 37°C, taken as reference since it is the average human body temperature. The temperature profile of the water heater taken from the data is presented in Figure 28. The temperature threshold values mentioned are visible from the graph, in particular the temperature goes above 50°C only in presence of photovoltaic production.

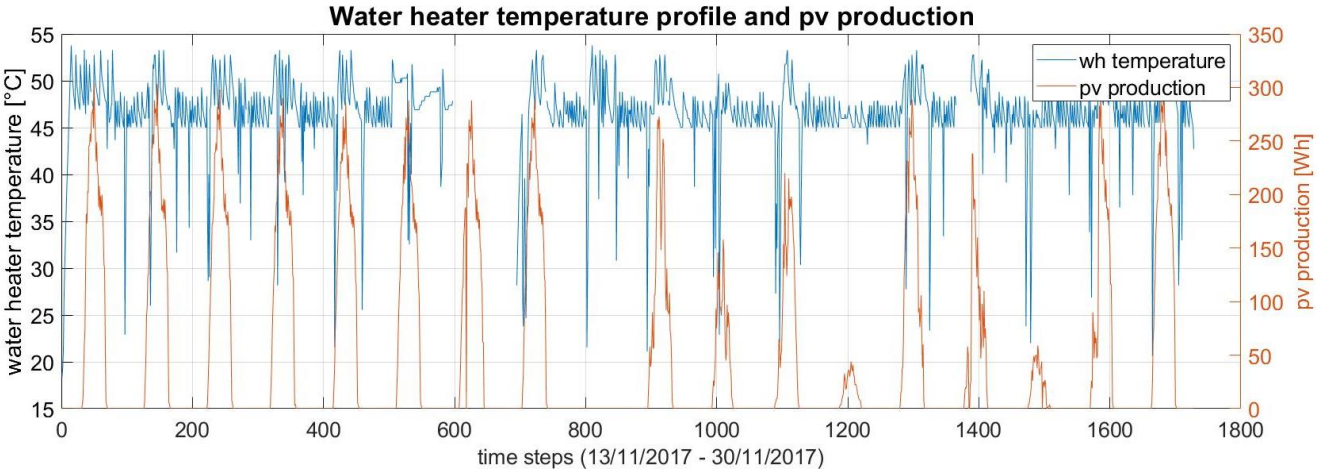

Figure 28: Temperature profile of the water heater and pv production

The total number of counted events is 879 showers in 361 days, corresponding to an average of 2.5 showers per day. Furthermore, the specific hours at which the event occurs have been collected and the resulting distribution is presented in Figure 29.

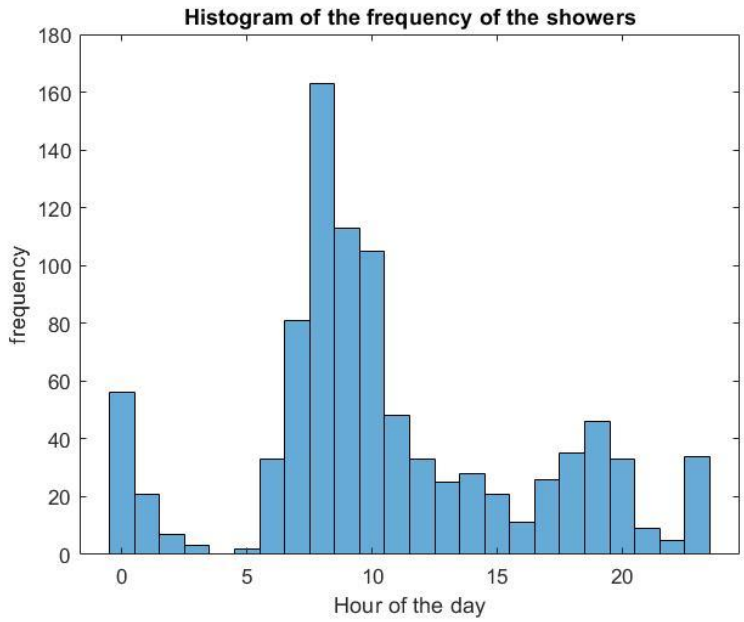

Figure 29: Distribution of the showers during the day from data

To recreate a thermal load curve, a random generator of load has been implemented. The first randomization concerns the number of showers per day: this value can be either 2 or 3 with the same probability, so on the long run the average will be 2.5 events per day. The second randomization concerns the hour at which the shower is taken. From the histogram of the frequencies, a cumulative distribution can be drawn, where the length of the segment is proportional to the probability of having the shower at that specific hour. The randomization will pick up a number between 0 and 1 and select the hour correspondent to the range of values. The cumulative function is presented in Figure 30.

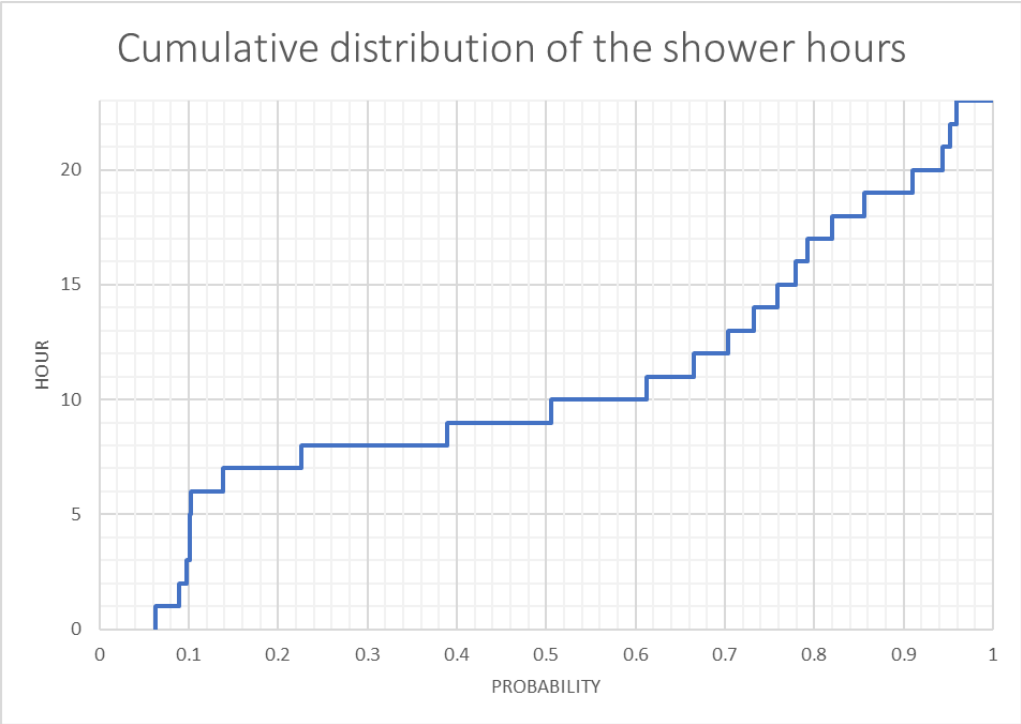

Figure 30: Cumulative distribution function of the even shower

The results of the model are here presented. The algorithm created a time series of 360 days, where the shower times follow the 893 showers, 2.47 per day on average. The distribution in the hours of the day has been re-evaluated from the new time series and it is shown in Figure 31:

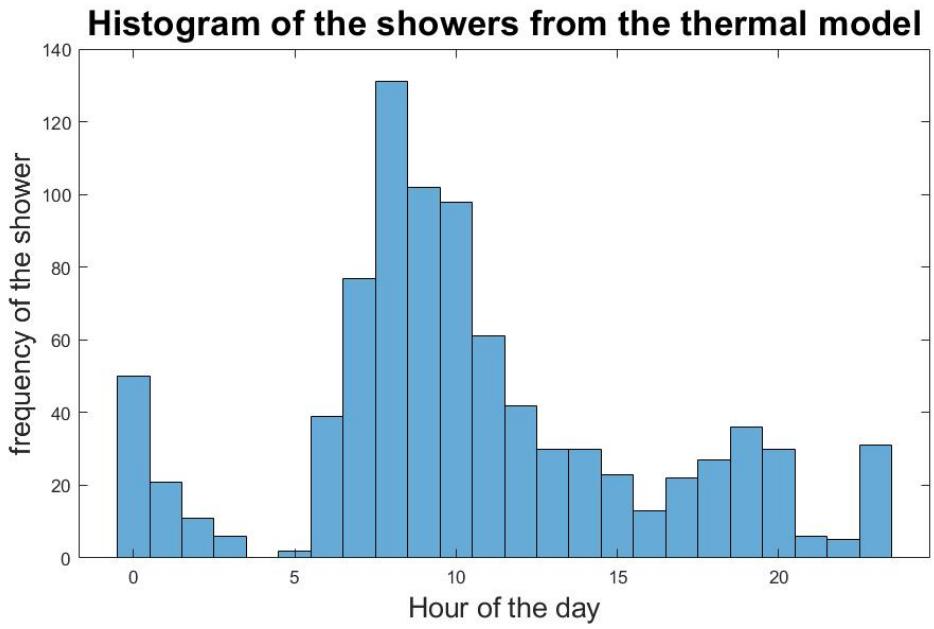

Figure 31: Histogram of the showers from the thermal model

The temperature profile produced by the algorithm is presented in Figure 32.

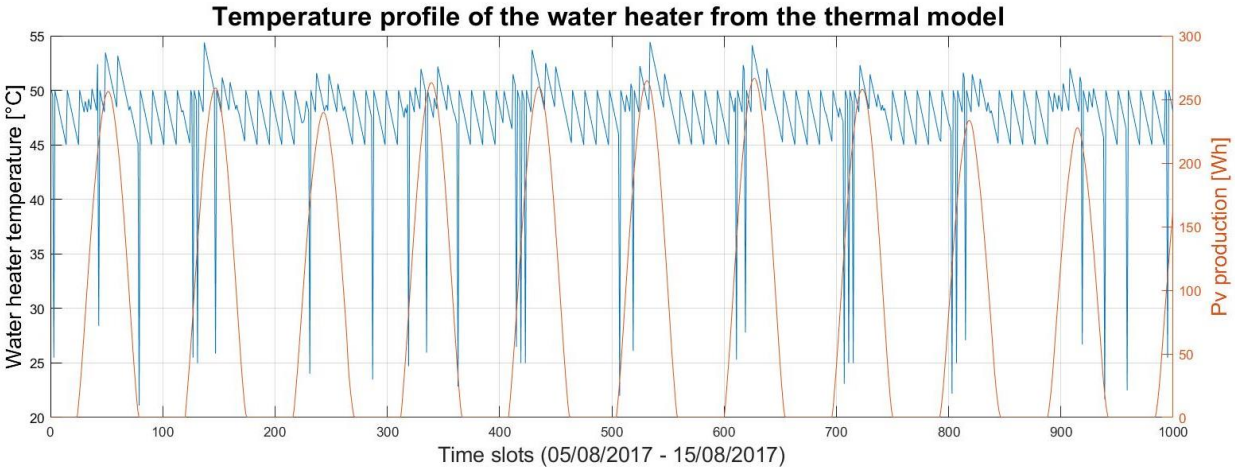

Figure 32: Temperature profile of the water heater produced by the algorithm

The final validation of the thermal model comes from the cumulative results. The total electricity input of the water heater of the model is 1.69 MWh_{el}, while the value from the time series is 1.66 MWh_{el} (ratio: 101.9%). The total thermal losses produced by the model are restored with 0.16 MWh_{el}, representing 9.7 % of the total water heater charge. This number is realistic and in line with the expected performance of the water heater.

4.4.4 Electric load modelling

The electric load modelling presented in paragraph 2.5 has been implemented and tested. However, the model did not produce satisfactory results to be validated. A very simple methodology has been applied to forecast the load, by simply using the average values for the month considered, keeping into account an average for the weekdays and an average for the weekends. Regarding the electric load used as input in the model, the timeseries have been imported as extracted from the dataset. More information on how the model has been implemented are available in Annex IV: Electric Load Modelling

4.4.5 Model of the battery

The roundtrip efficiency of the battery from the technical details of the manufacturer is 95%. The lifetime of the battery depends on the maximum number of cycles that the battery can withstand. One way to estimate the battery degradation can be to consider the warranty time (10 years), assuming 1 cycle per day and linear degradation, and finding a maximum number of cycles of 3650 [6]. In the model, having a 15-minutes based timestep, the technical constraint of the maximum power that the battery can deliver or absorb results in 750 Wh. The panoramic of the technical parameters of the battery is available in Table 10.

Table 10: Battery technical parameters and inputs

symbol	Name	Value - Formula
B_c	Battery capacity	3.3 kWh
B_{max}	Maximum power	3 kW
B_{eff}	Usable energy	3 kWh
μ_b	Round trip battery efficiency	95 %
N_{max}	Number of charge/discharge cycles	3650

5 Results

5.1 Technical Performance Results

5.1.1 Analysis of the performance from time series

The performance of the HMS can be estimated from the time series of the dataset by calculating some parameters for the different customers. The goal of the maximization of the self-consumption is achieved when the household consumes electricity mostly from the photovoltaic panel and the interaction with the grid is minimized, considering both purchase and injection.

The photovoltaic electricity generation is managed by the HMS during the period August 2017 - August 2018. The system worked according to the algorithm presented in Figure 33.

Figure 33: HMS prioritization of the electricity generated by the photovoltaic panel

5.1.2 Self-Consumption Ratio

The average SCR of the customers is 57.23 %. The value results particularly high for the customers that have the largest electricity consumption, or customers that consumes most of the electricity during the daytime. A very high Self-Consumption Ratio can be a sign that the photovoltaic system is undersized for the energy needs of the households. An overview for the customers of Valverde is presented in Figure 34.

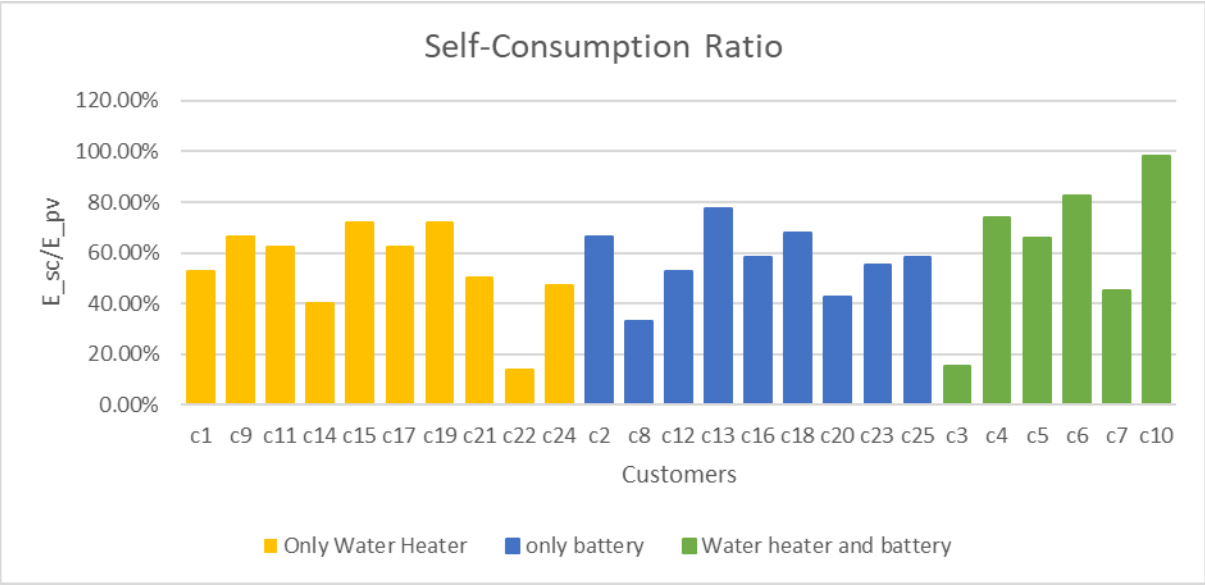

Figure 34: Self-Consumption Ratio summary

Customer 10 has the highest electricity consumption and manages to absorb almost all the electricity supplied by the photovoltaic panel.

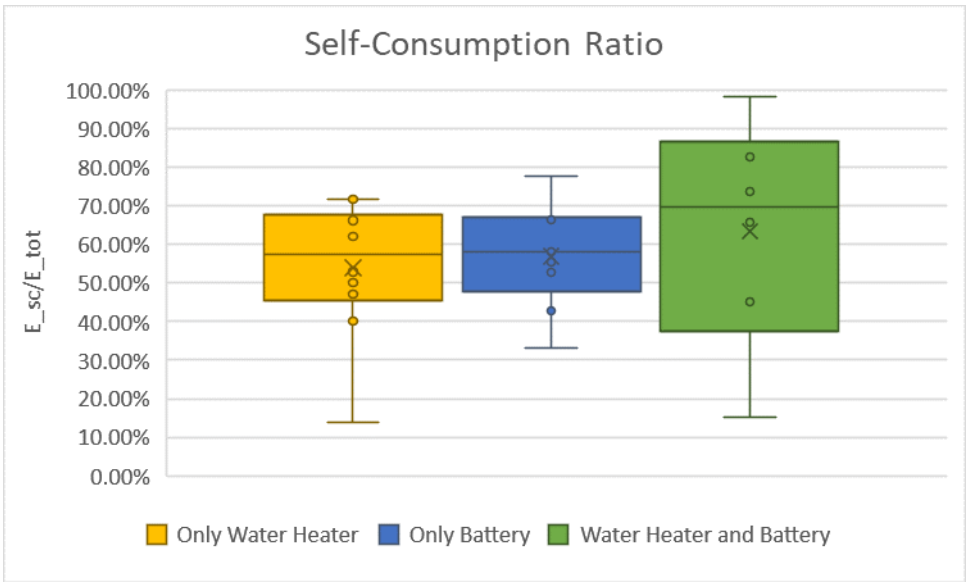

Figure 35: Boxplots of the Self-Consumption Ratios for the three different configurations

The highest SCR is achieved by the complete configuration, but in general the three configurations are comparable in terms of SCR performance.

5.1.3 Self-Sufficiency Ratio

The average SSR of the customers is 31.16%, with a minimum of 5.46% for customer 22 and a maximum of 54.46% for customer 12. A summary is available in Figure 36.

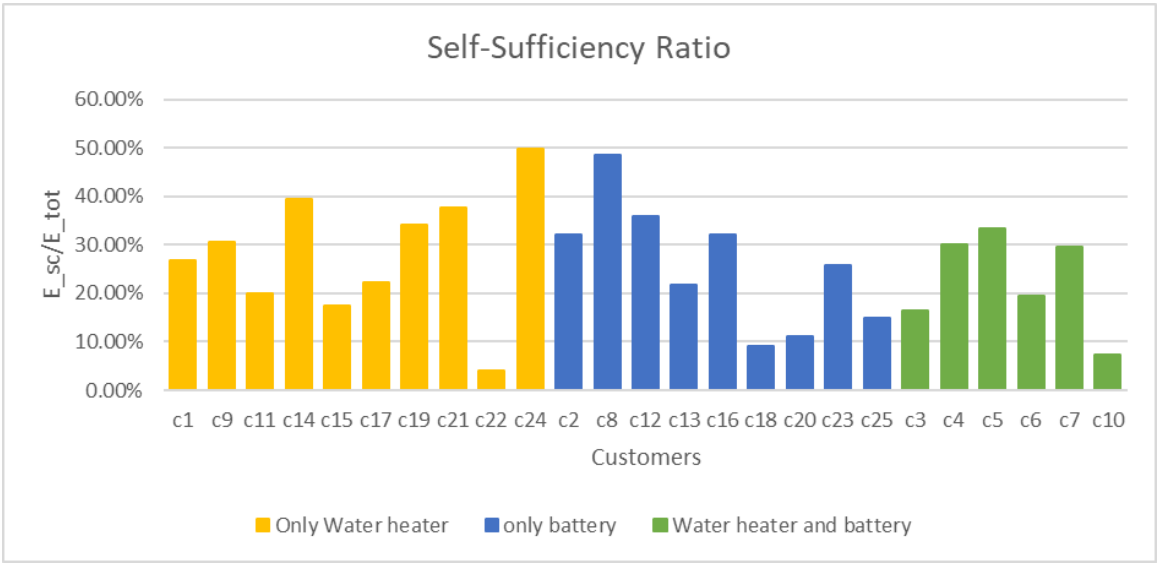

Figure 36: Self-Sufficiency Ratio summary

As expected, considering the three different configurations available, the best performance in terms of SSR is achieved by the consumers having the smallest electricity demand, and the worst performance by the customers with the highest consumption, due to the fact that the panel has always the same size.

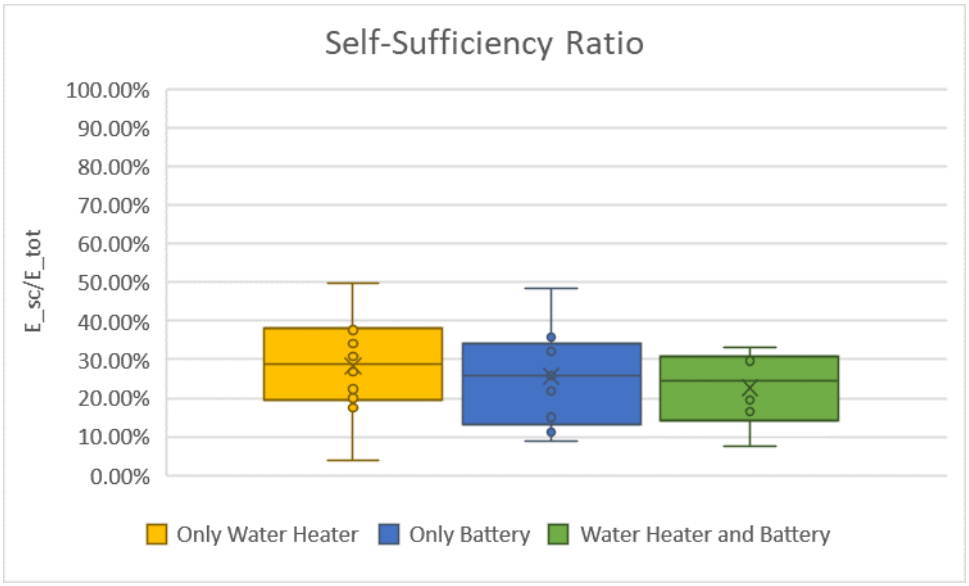

Figure 37: Boxplots of the Self-Sufficiency Ratios for the three different configurations

Customer 10 has a very limited SSR and a strong influence on the distribution of SSR for the configuration with water heater and battery. For this reason, the performance of the complete configuration results worse than the case with the water heater only. It must be mentioned that the number of customers analysed has a strong influence in general on the statistical significance of the benchmark among the configurations.

5.1.4 Combination of SCR and SSR to analyse the system

Observing the two parameters together, SCR and SSR some observations and comments on the effectiveness of the system installed are possible:

- High SCR and low SSR: the customer absorbs most of the photovoltaic energy, but this is not enough to cover a considerable part of the demand. The system is undersized. Customers 10 and 18 are examples.
- Low SCR and high SSR: the customer consumes a limited part of the electricity from the panel, but this is enough to satisfy a considerable share of the demand. The system is oversized. C8 is an example.
- High SCR and SSR: the customer absorbs most of the photovoltaic energy and his demand is highly satisfied. The system has a very high performance and it's properly sized. Customers 5, 14 and 24 are examples.
- Low SCR and SSR: the customer is not able to properly use the electricity from the panel, this can be due to a consumption mainly shifted during night time. In this case, the battery could be undersized, installing a larger capacity could be an option.

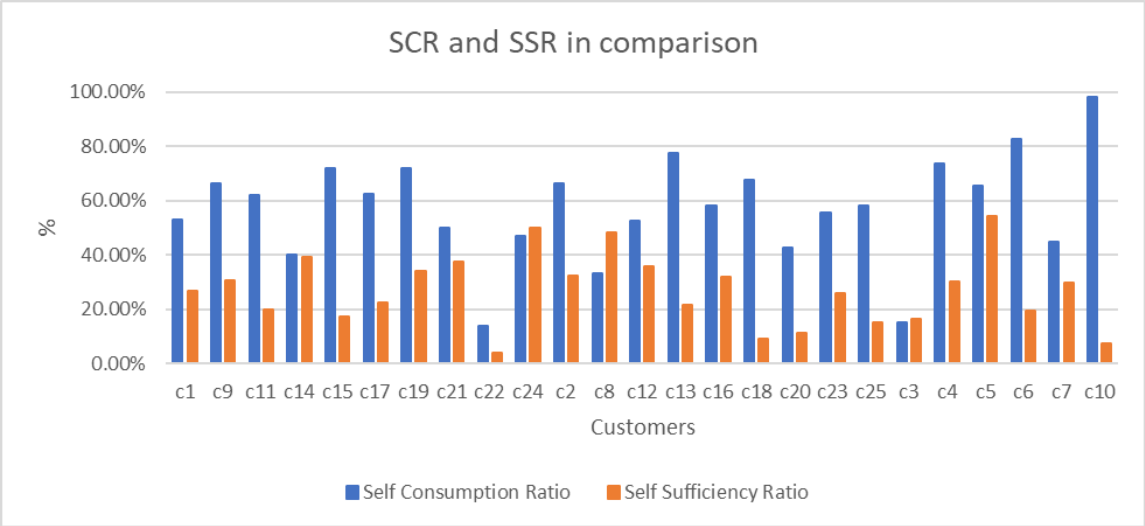

Figure 38: Cross-comparison of SCR and SSR

For instance, customer 3 has almost 75% of the consumption concentrated between 7 PM and 8 AM, so we can consider it a night consumer. Even though a battery is installed, it is not enough to achieve a high performance of the system, the demand is too much shifted in the night hours.

5.2 Economic performance results

The savings on the electricity bill are strictly related to the Self-Sufficiency and Self-Consumption Ratio. The calculation of the savings is performed based on the methodology presented in 4.3.2. The savings are what actually makes the project interesting for the end customers. An overview is presented in Figure 39.

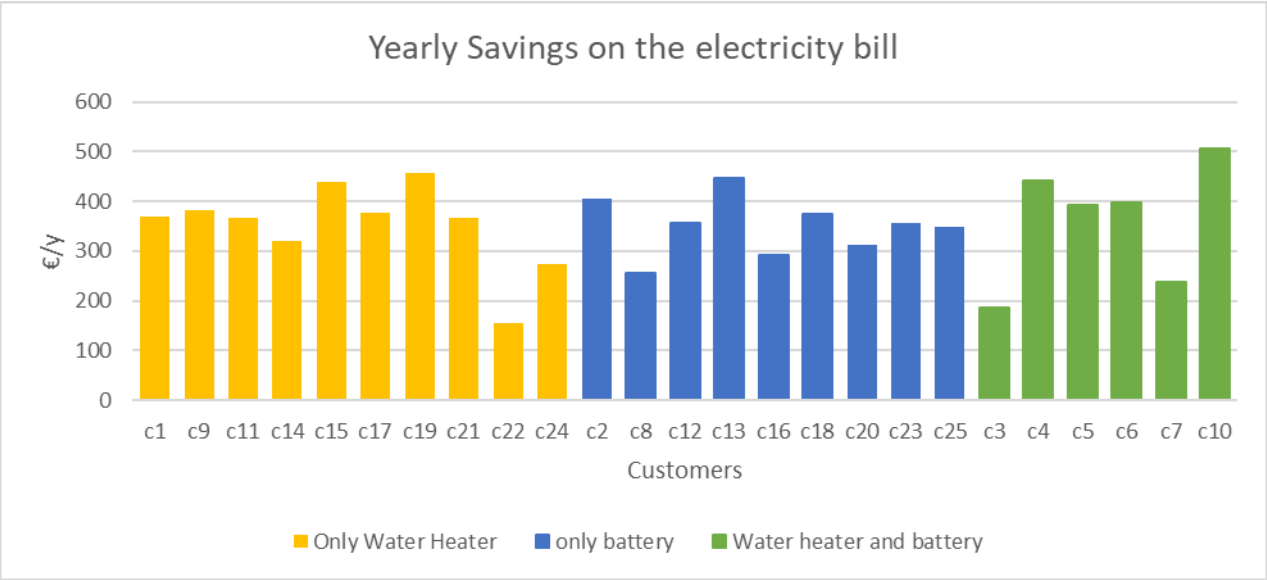

Figure 39: Total savings on the electricity bill

In absolute terms, all the customers have a significant benefit out of the project. The average savings are estimated to be 352 €/ year for each customer, corresponding to an average monthly saving of 29 €/month. This value is very close to the estimation made by EDP, which is around 25 €/month. [29] A summary of the relative savings is presented in Figure 40.

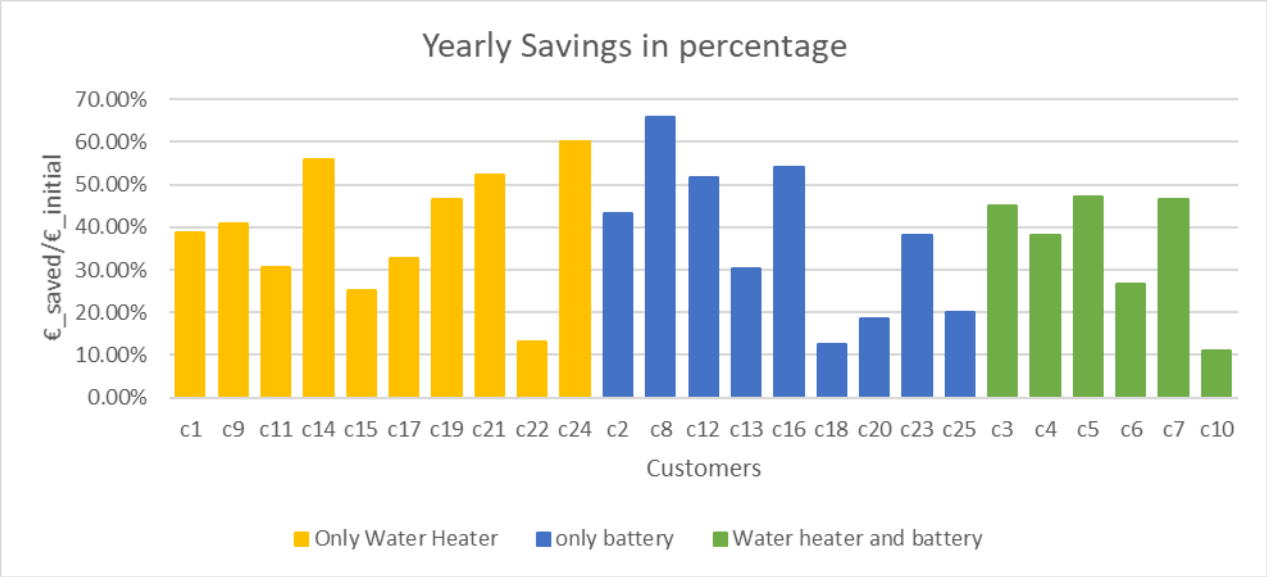

Figure 40: Percentage of savings on the electricity bill, calculated as the savings divided the original bill

The customers with the smallest relative benefits are customer 10 and 18, the ones with the largest electricity demand. In general, the performance of the installation depends on three factors:

- The size of the equipment compared to the electricity demand (under sizing - oversizing);
- The configuration of the equipment installed;
- The distribution of the electric load during the day and the night.

The correlation between relative savings and electricity demand is negative. This trend is clearly visible in Figure 41. This is due to the fact that every customer has the same size of the photovoltaic panel, that is undersized for the largest consumers like customer 10.

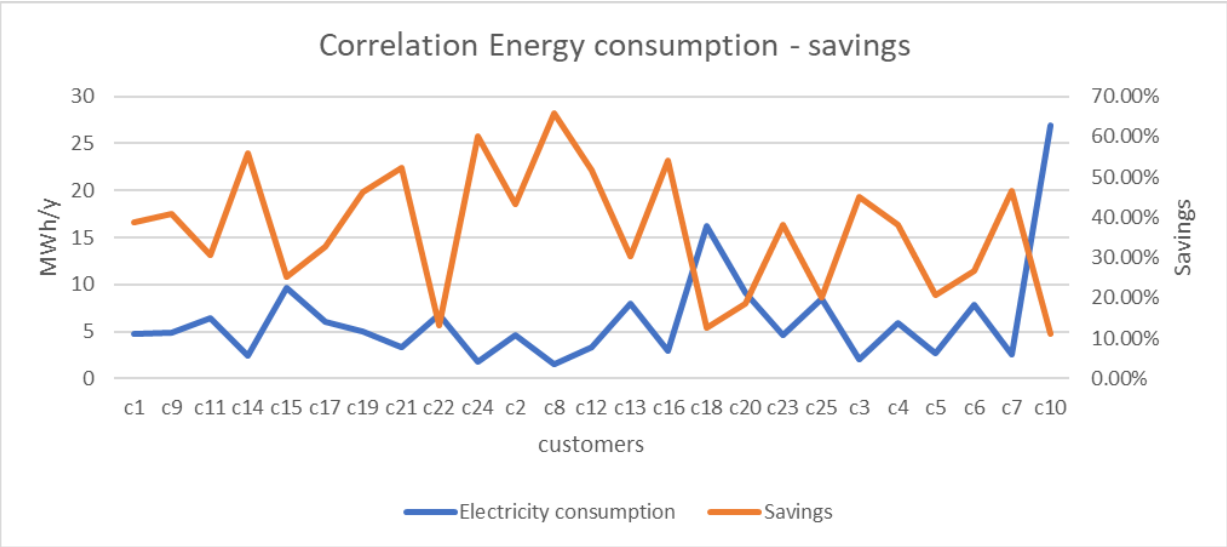

Figure 41: Correlation between electricity demand and savings on the bill

The same trend is visible in the Scatter Plot presented in Figure 42.

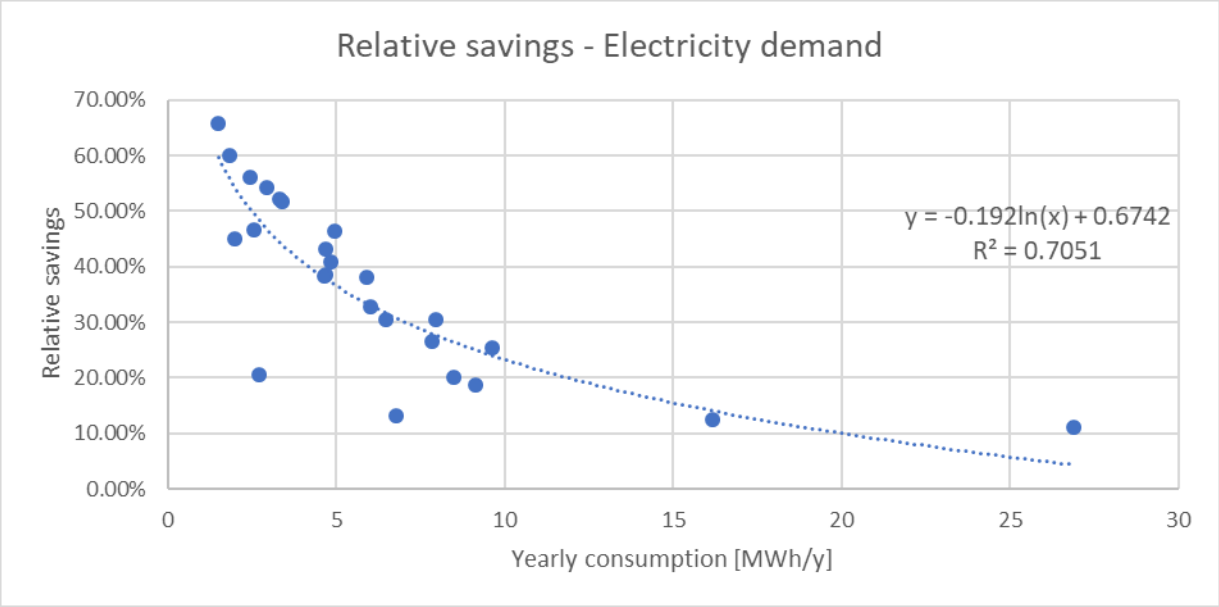

Figure 42: Scatter Plot of the relative savings, function of the yearly electricity demand

For customers having a considerable amount of electricity consumed during the night, the benefits of the photovoltaic panel will be lower. The savings will be even less significant if the panel is undersized for the specific needs of the customer.

Comparing the three configurations, adding the battery to the water heater only doesn't bring significant changes: the average differs of 0.15%, slightly in advantage of the complete configuration. The configuration with battery only has a significantly lower value, 35.14%. The boxplots are presented in Figure 43.

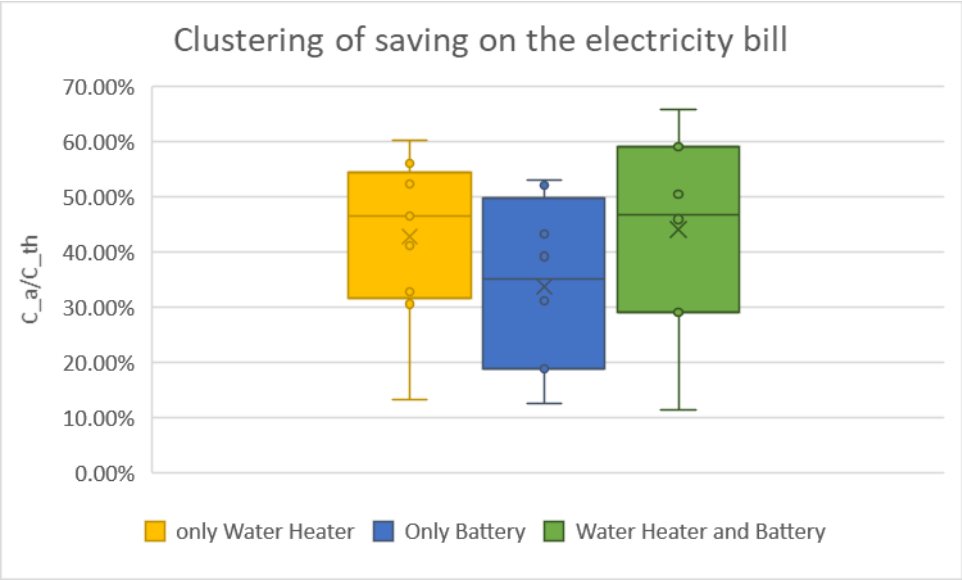

Figure 43: Boxplots of the savings on the bill for the three configurations.

It is important to mention that the savings for the configuration with battery only don't include any calculation on the thermal consumption and expenditure. The customers having only the battery are probably using natural gas to heat the water up, and this cost is not considered in this calculation.

5.3 Model results

5.3.1 Validation of the working principle

The objective of the simulation is to compare the performance of the current configuration of the Home Management System with new algorithms. The main inputs of the model are listed in Table 11.

Table 11: Main inputs of the model

Main inputs	
Solar Radiation	CAMS radiation service
Photovoltaic generation	Perez Model and Pv details
Electric load	Customer 5 timeseries
Thermal load	Randomization model
Solar forecasts	Similarity model
Load forecasts	Average monthly load
Water Heater	
Average Water consumption load	45 litres
Tmin	45°C
Tmax (grid)	50°C
Tmax (solar energy)	53 °C

The model should replicate approximately the behaviour of customer 5. A first simulation has been performed to check the representativeness of the model, so the time series of the photovoltaic generation have been used. The main results are shown in Table 12

Table 12: Model results compared with the data

Parameter	Values from the model	Values from timeseries
Total Electricity Purchase	2.82 MWh	3.11 MWh
Total Electricity Injection	0.70 MWh	0.66 MWh
Total WH charge	1.69 MWh	1.61 MWh
SSR	35 %	52 %
SCR	68 %	66 %

The model presents a discrete level of accuracy, but some issues appear in the estimation of the electricity injected to the grid. The validation of the thermal model with the water heater input data has already been presented in paragraph 0.

The working principle of the algorithm appears correct and some graphs are presented to show that the main technical constraints of the HMS are respected.

The temperature of the water heater goes above 50°C exploiting thermal flexibility only when excess electricity from the photovoltaic panel is available. The temperature profile in relation with the pv production is visible in Figure 44.

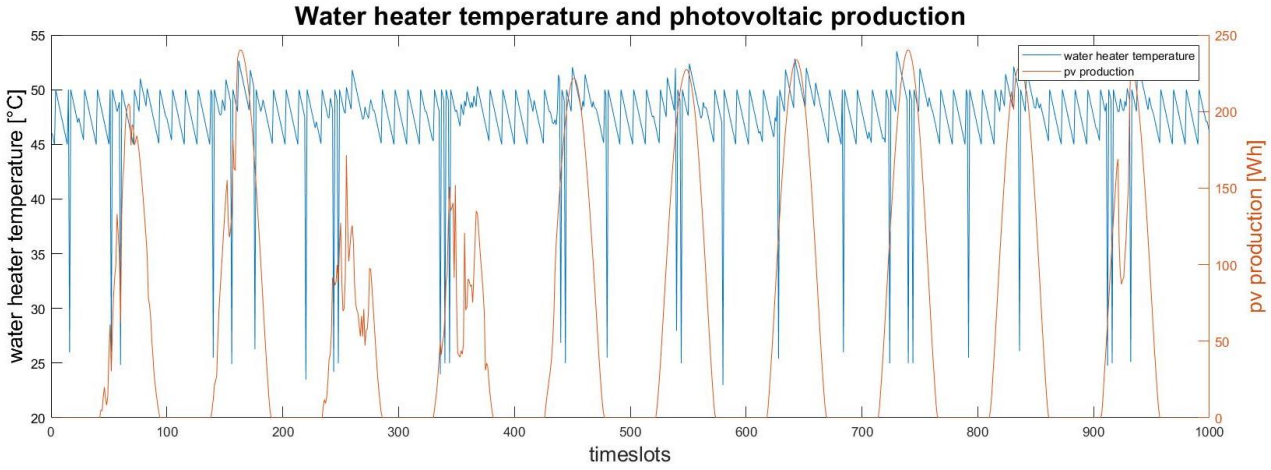

Figure 44: Water heater temperature and photovoltaic production from the model

The HMS only charges the battery in presence of photovoltaic energy, and not with the grid, as shown in Figure 45.

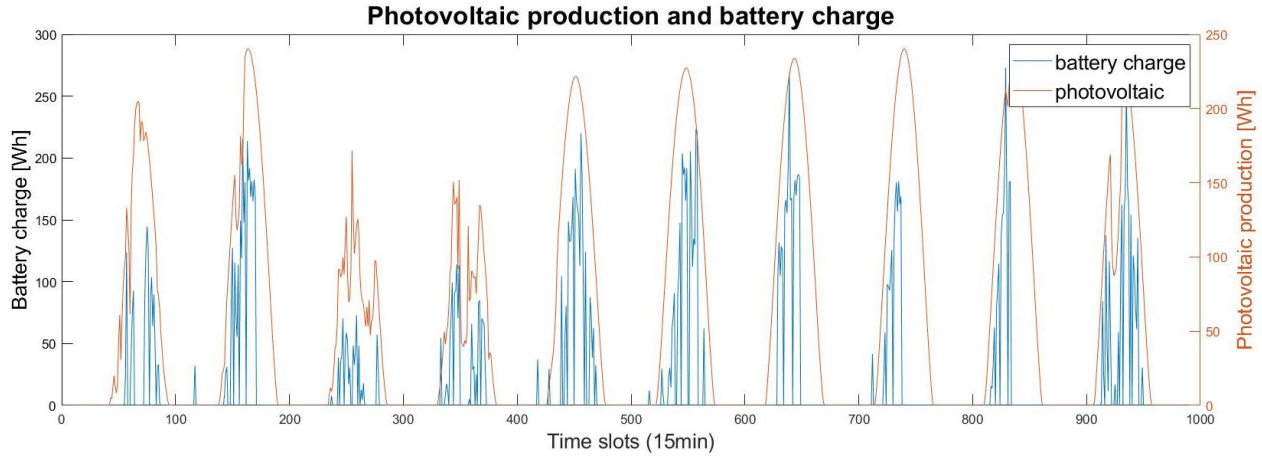

Figure 45: Photovoltaic production and battery charge from the model

The excess electricity is injected only when the battery reaches 100% of the state of charge. This is visible in Figure 46.

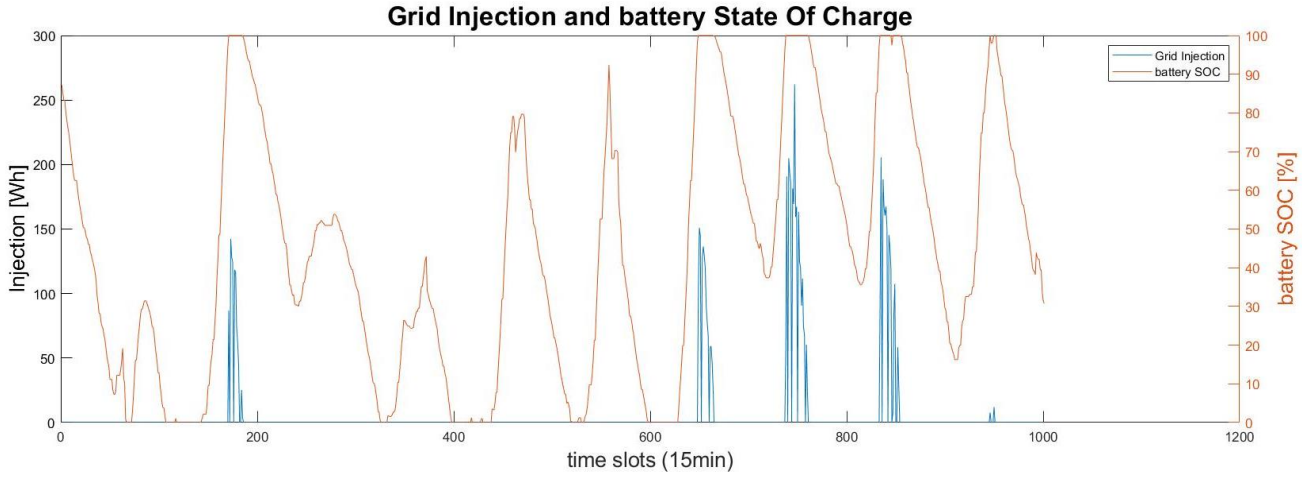

Figure 46: Grid injection and battery SOC from the model

5.3.2 Implementation of the new HMS

The implementation of the new algorithm for the HMS follows the scheme presented in Figure 47. The general idea is to trigger some night charges of the battery, to take advantage of the cheaper electricity price. First the user decides a triggering criterion of activation, starting from the weather and load forecasts. Then a charging criterion for the battery is set, to decide how much of the capacity of the battery should be recharged for every activation. The algorithm verifies the triggering criterion every day at midnight: when the criterion is met, the battery is charged up to the desired capacity with the electricity coming from the grid.

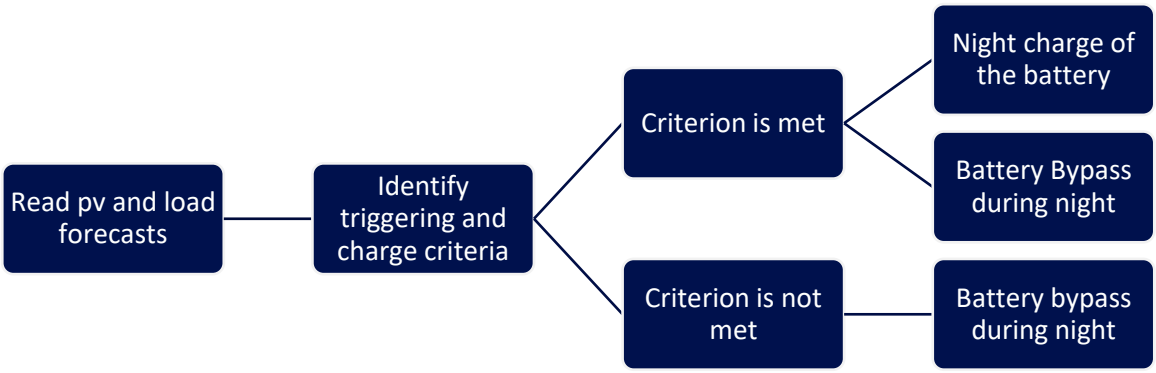

Figure 47: New algorithm for the HMS

The new algorithm is expected to increase the number of cycles that the battery does every year, and to shift part of the demand from the day to the night, having a time-of-use tariff. For technical reasons, it is better to keep the number of cycles of the battery around one per day maximum. This should preserve the lifetime of the battery within the time boundaries mentioned.

Since most of the inputs come from derived variables, and the photovoltaic data derive from the satellite radiation database, the results are realistic but will be analysed mostly in comparative terms among the model results of the base case and the new algorithm.

Several strategies of triggering and charge criteria have been tested. The main criterion consists in comparing the forecast of the photovoltaic electricity production with the load forecast. If the daily load forecast is higher than the daily photovoltaic generation forecast, the algorithm charges the battery during the night of a specific percentage, settable to different values.

$$Eq. \qquad E_{dtot,day} > E_{pv,day} \cdot N \qquad (38)$$

Where N is an additional multiplicator of the electricity production. The different tested strategies are shown in Table 13. Also, a battery bypass is implemented to prevent the discharge during off-peak hours: in this way, the battery only delivers electricity during the period when the tariff is higher.

Table 13: Strategies tried to improve the results of the HMS

Strategy	Night Bypass	PV multiplicator N	Battery Charge
S1	Yes	x1	0%
S2	Yes	X1	50%
S3	Yes	x2	100%
S4	Yes	x2	50%
S5	Yes	x2.5	50%
S6	No	x1	100%
S7	No	x1	50%
S8	No	x1.5	50%

For instance, for strategy S3 the algorithm verifies if the daily electric load is going to be at least twice the photovoltaic generation: in that case, during the night the HMS charges the battery up to the full capacity (100%) and it's not going to discharge the battery during off peak hours.

The final results are not bringing improvements to the original algorithm in terms of savings on the electricity bill. The results are shown in Figure 48, where the original algorithm shows a better performance than the other tested strategies.

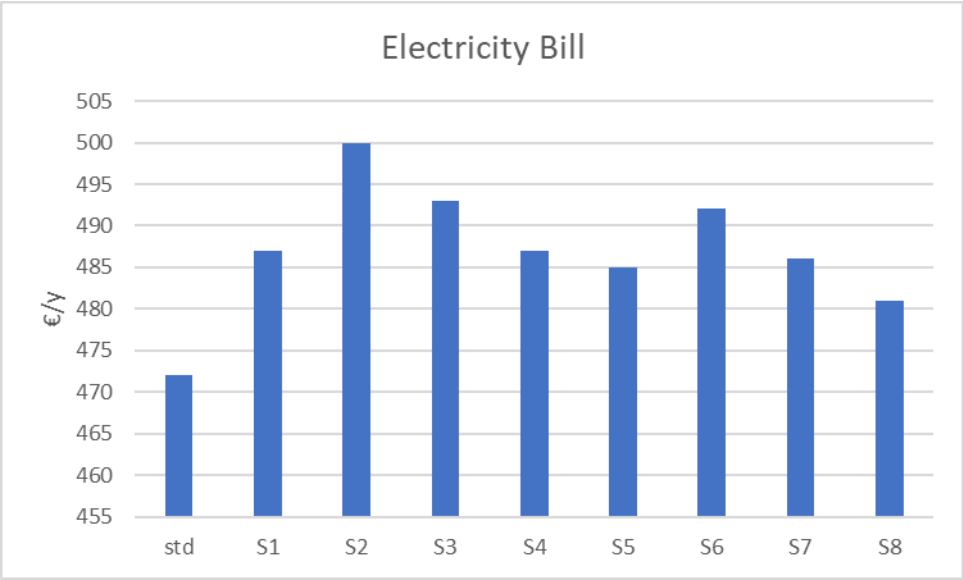

Figure 48: Final results for the electricity bill after the application of the different strategies

The reasons can be several:

- Poor performance of the load forecast;
- Poor performance of the weather forecast;
- The choice of comparing the electric load and the pv production only is not enough, the thermal demand should also be included

The model manages to shift part of the electric load during the night. However, the effect of this shift is negatively compensated by an increase of the electricity purchased from the grid. The overall result is that it's not convenient to apply the proposed scheme.

Additional strategies not investigated in this work could have a positive impact for the end customers.

6 Conclusions

SENSIBLE project is successful relatively to the initial goals of creating a more independent group of customers, self-consuming a considerable amount of electricity and saving more than 100 euros per year on average. The work focused mainly on the perspective of the end customer and did not analyse the detail of the grid dynamics. For further studies many possibilities are open, both to improve what has been done in this report and to analyse a different perspective. Possibilities to explore are:

- A more advanced thermal model for the water heater, for instance including a stratification model or changing the approach into a black-box model, for instance using a neural network to set the parameters;
- A model that keeps into account the interactions among houses;
- More advanced weather and load forecasts;
- An analysis of how the battery of the end customer can be controlled by aggregators to provide balancing services.

6.1 Suggestions

According to the criteria mentioned in paragraph 5.1.4, some indications are given to understand if the equipment installed is suitable for the type of customer or not. It should be noticed that, even though most of the customers would benefit from a more photovoltaic panel capacity, the size of 1.5 kW was chosen to avoid the necessity for additional permissions for the installation. An overview is presented in Table 14.

Table 14: Suggested interventions for the customers

Customer	Intervention
C1	Increase PV size
C2	Increase PV size
C3	Increase size battery
C4	Increase PV size
C5	Good sizing
C6	Increase PV size
C7	Increase PV size
C8	System slightly oversized
C9	Increase PV size
C10	Increase PV size
C11	Increase PV size
C12	Good sizing
C13	Increase PV size
C14	Good sizing
C15	Increase PV size
C16	Good sizing
C17	Increase PV size
C18	Increase PV size
C19	Increase PV size
C20	Increase PV size
C21	Good sizing
C22	Increase size battery
C23	Increase PV size
C24	Good sizing
C25	Increase PV size

6.2 Financial feasibility and perspectives

The CAPEX of the installations in SENSIBLE has been paid by EDP, but the project wants to investigate the financial sustainability of the distributed generation and storage for residential customers in Portugal. A financial assessment can be performed starting from the investment costs of the devices installed, and considering the savings calculated for the current year as a starting point for the incoming years. The financial parameters used for the analysis are the Net Present Value NPV in equation 39 and the Internal Rate of Return IRR.

Eq.
$$NPV = \sum_{j=1}^{n} \frac{(CF_j)}{(1+i)^j} \tag{39}$$

It is reasonable to assume that the savings will decrease during the years, due to the degradation of the components. A good assumption is to decrease savings proportionally to the degradation of the photovoltaic panel cells. The GreenTriplex PM060P00 is a Multi-Chrystalline photovoltaic module, and the performance is guaranteed with linear degradation to 80% of the rated power for 25 years. Normally the initial degradation of the panel is higher, and then it stabilizes on a linear trend, so to have a more conservative result, the degradation will be assumed to be:

- -5% for the first year;
- -0.63% for the following years.

The yearly savings due to the battery can be estimated as the electricity delivered by the battery as if it was delivered by the grid, with the correspondent time of use tariff.

Eq.
$$B_{batt} = \sum_{i=1}^{x} 0.0969 \cdot E_{b,out,i} + \sum_{j=1}^{y} 0.2028 \cdot E_{b,out,j} \tag{40}$$

Where:

- $E_{b,out,i}$ is the battery output in off-peak hours;
- $E_{b,out,j}$ is the battery output in peak hours.

The average savings due to the battery are around 77 €/year. The results are presented in Figure 49.

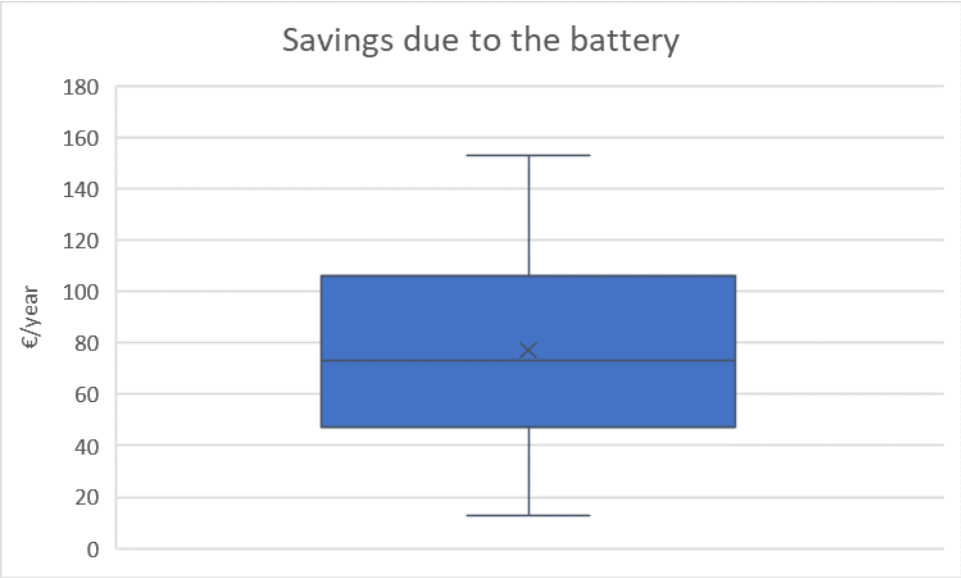

Figure 49: Boxplot of the yearly savings thanks to the battery

The financial inputs are presented in Table 15. The interest rate suggested by EDP for the calculations is 6%, and the lifetime considered for the project is assumed to be 20 years.

The savings on the electricity bill are considered positive values in the cash flow calculation.

Table 15: Financial inputs

Device	CAPEX [€]	OPEX [€/y]	Lifespan [y]
Photovoltaic panel and inverter	1500	20	20
Smart Water Heater	800	-	20
Battery	2550	10	10
Battery inverter	500		20

With the mentioned values, two cases can be analysed: the case with the battery and the case without the battery. The savings with the water heater have been assumed to be 350 €/year, value taken from the average of the savings of the customers with this configuration.

The NPV is calculated on a lifetime of 20 years. The battery must be replaced after 10 years, so it will be accounted twice, while the PV and the Water Heater are accounted once.

The cumulative actualized cash flows for a customer without the battery are presented in Figure 50. From the figure the Payback time is in year 9. The NPV is 1374 € in year 20, however the equipment is expected to last for longer, at least five more years. The IRR is 14.7%

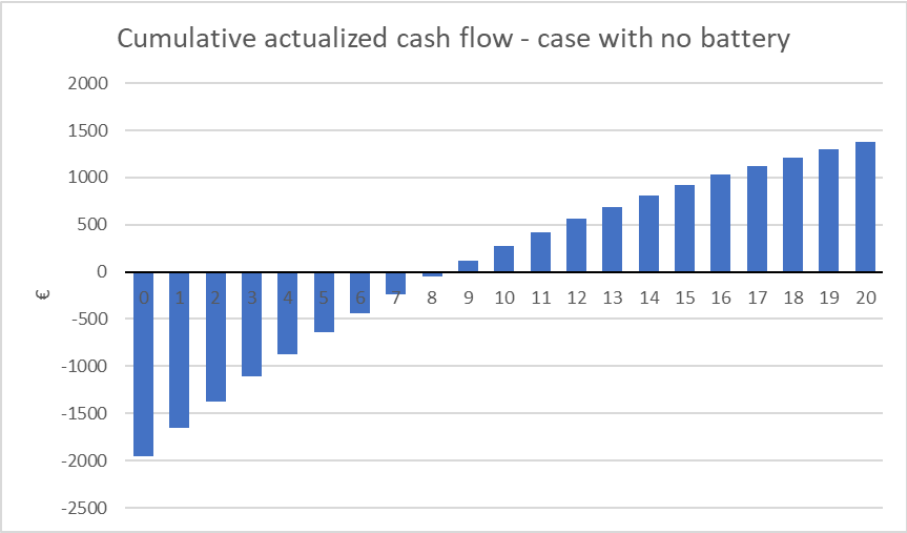

Figure 50: Cumulative cash flow of the case without battery

Considering the case with the battery included, a second inverter is necessary, so the investment cost is expected to grow. The cash flows are shown in Figure 51. A replacement of the battery is considered in year 10. The NPV and the IRR are negative, with a value of the latter of -0.85%. This means that the investment is not sustainable at the moment with the current prices of the battery.

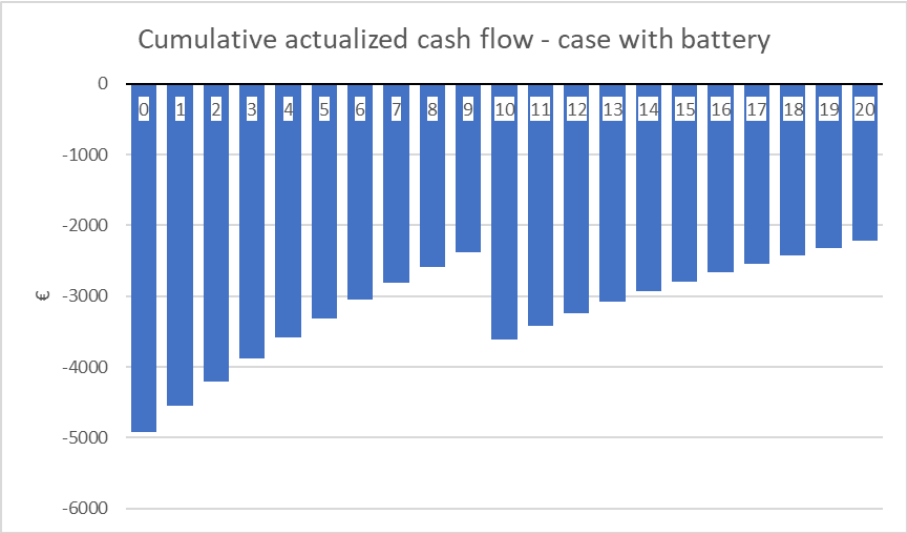

Figure 51: Cumulative actualized cash flow of the case with the battery

The financial analysis suggests that the battery is not a convenient investment for the current values of CAPEX and interest rate. However, it is possible to identify the CAPEX that would make the investment neutral, which is 1125 € (340 €/kWh).

It is interesting to notice that the price of the selected battery, 772 €/kWh is very high for the current market prices: The cost of a Tesla Powerwall 3 of 24 kWh is approximately 10000 $, corresponding to 435 USD/kWh. [35] The battery market in Portugal is still not developed, and for this reason mainly the cost per kWh installed is still not affordable for a domestic installation.

According to a study of HIS Markit, the price of lithium ion batteries could fall below 200 $/kWh, 174 €/kWh. [36]

Another interesting aspect to be considered is that the general trend of the prices of electricity in Portugal is growing: even though in the three semesters between the end of 2016 – end of 2017 the price slightly decreased, from 2010 to the end of 2017 the prices increased of 41%, corresponding on average to a 6% increase per year. The graph presented in Figure 52: Electricity prices for households in Portugal from 2010 to 2017, semi-annually (in euro cents per kilowatt-hour) Figure 52 is taken from Statista [37] and shows the mentioned trend.

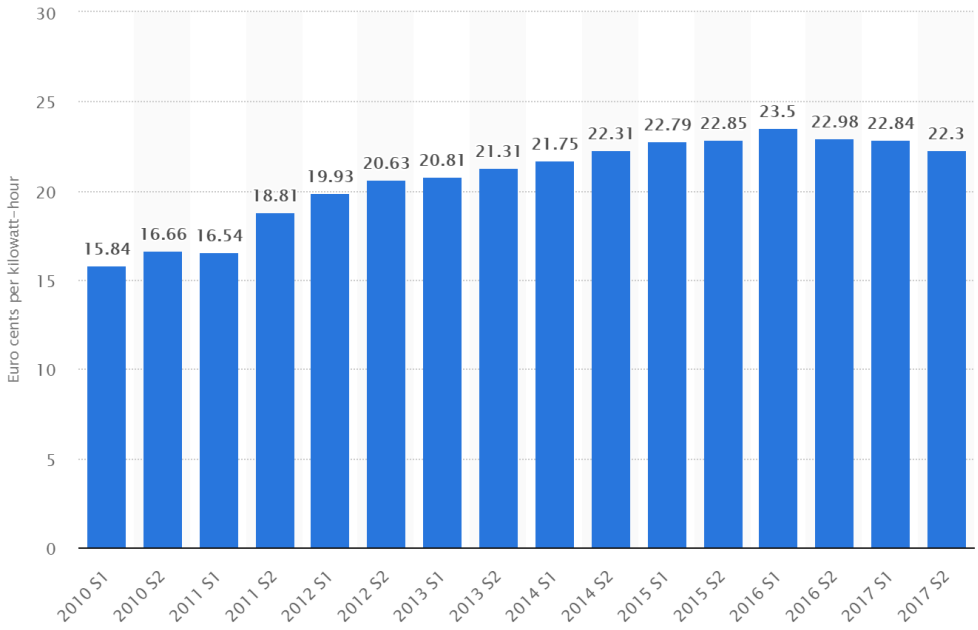

Figure 52: Electricity prices for households in Portugal from 2010 to 2017, semi-annually (in euro cents per kilowatt-hour)

The growth in the electricity cost might partially mitigate the savings reduction due to the degradation of the equipment and make the investment more convenient. Even though there is a probability that this will have a positive impact in the financial perspectives of the installation of such systems, an accurate evaluation at this stage would be merely speculative and it is not performed for reasons of conservativity.

6.3 Impact of the project

6.3.1 Environmental impact: Carbon Footprint

The carbon intensity of the electricity production can be defined as:

$$CI = \frac{GHG_e}{E_{gen}} \quad \text{Eq.} \quad (41)$$

Where:

- GHG_e is the total emission of greenhouse gasses, expressed in tons of CO_2 equivalent;
- E_{gen} is the total electricity generated

The greenhouse gasses emissions of the electricity supplied by the grid are due generation, but also many other intermediate steps before the final energy consumption by the end customer.

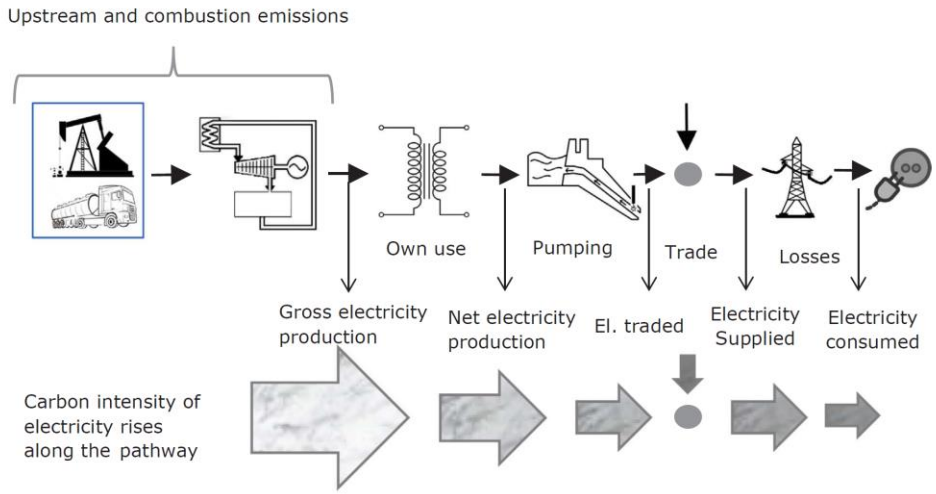

Figure 53: Evolution of the carbon intensity along the electricity supply chain [38]

The carbon intensity of the national grid of Portugal can be assumed to be 400 g $CO_{2,\,eq}$/kWh consumed by the end customer. [38] A similar value is found on the website of the Electricity Map, where live values of the carbon intensity of the grid are shown [39]. The electricity self-consumed by the customers of Valverde totals 27134.97 kWh, corresponding to a reduction of the emissions of 10.85 tonnes of CO_2 equivalent in the period August 2017 – July 2018. It must be mentioned that in this calculation the emissions related to the installation and maintenance of the system and related to the manufacturing of the components are not accounted. A life-cycle assessment of the project SENSIBLE from Cradle-to-Grave would give a complete overview of the mentioned aspects, and it is an interesting hint for further studies on the performance of the project.

6.3.2 Socioeconomic Impact

Distributed generation in general gives positive impact to the management of the grid. For instance, a reduction of the losses, improved reliability of the grid by reducing power flows, more free capacity available on the power lines, an increased renewable penetration in the domestic energy consumption. [40] The electric systems worldwide are experiencing a very fast evolution first with the introduction of large renewable power plants, and now with distributed generation. SENSIBLE project is just one of the case studies where batteries are combined

with photovoltaic for domestic use. Some companies already commercialize domestic batteries in countries where the market is larger, such as the US.

Having a high number of customers getting more and more independent from the grid is expected to lead to a reduction in the earnings of the DSO, because less electricity is purchased. Nevertheless, the grid will still be needed to supply the customers when renewables are not available, for instance during the night, or in cloudy days. The costs of maintenance of the grid will have to be recovered by the grid operators. Furthermore, the investments in the grid are usually very long term oriented, planned to be recovered in decades, while the peak load profile changes at an increasing speed.

If the grid costs increase and the price of electricity grows consequently, some problems of disparity in the redistribution of the costs might appear. Usually grid costs are higher in rural areas, where there is space available for rooftop photovoltaic installation: Valverde is a good example. With more and more affordable batteries and photovoltaic panels, more customers are expected to become prosumers, increasing the renewable penetration in areas where the consumption is low. The combination of the two aspects is expected to considerably increase the grid costs and consequently the tariffs charged on the end customers. The most affected customers in this scenario would be the ones that cannot afford to install a solar system, generating an iniquitous trend in which the low-income households are disadvantaged.

An evolution of the current business model is expected to happen to mitigate this phenomenon. In fact, in a tariff where the customers are charged mostly on volumetric basis [€/kWh], customers having photovoltaic systems or in general private electricity generation would pay less than the customers totally dependent from the grid. [41] If grid tariffs are applied mostly on contracted power basis [€/(kWh d)] then the costs would be redistributed in a more fair and balanced way.

References

[1] United Nations, “Sustainable Development Goals,” 2015. [Online]. Available: https://www.un.org/sustainabledevelopment/sustainable-development-goals/.

[2] International Energy Agency, “Technology Roadmap: Smart Grids,” 2011. [Online]. Available: https://www-oecd-ilibrary-org.focus.lib.kth.se/docserver/9789264115071-en.pdf?expires=1529148090&id=id&accname=oid023441&checksum=1728299CF6309F0F845B6BF761A0360D.

[3] International Energy Agency, “Smart Grids: Tracking Clean Energy Progress,” 23 5 2018. [Online]. Available: https://www.iea.org/tcep/energyintegration/smartgrids/.

[4] International Energy Agency, “World Energy Outlook 2017,” 2017. [Online]. Available: https://webstore.iea.org/world-energy-outlook-2017.

[5] D. Neves and C. A. Silva, “Optimal electricity dispatch on isolated mini-grids using a demand response strategy for thermal storage backup with genetic algorithms,” 2015. [Online]. Available: https://www.sciencedirect.com/science/article/pii/S036054421500078X.

[6] G. Lorenzi and C. A. S. Silva, “Comparing demand response and battery storage to optimize self-consumption in PV systems,” 2016. [Online]. Available: https://www.sciencedirect.com/science/article/pii/S030626191631042X.

[7] M. F. Shaaban, A. H. Osman and M. S. Hassan, “Day-ahead Optimal Scheduling for Demand Side Management in Smart Grids,” 2016. [Online]. Available: https://ieeexplore.ieee.org/document/7920240/.

[8] I. Gupta, G. Anandini and M. Gupta, “An Hour wise device scheduling approach for Demand Side Management in Smart Grid using Particle Swarm Optimization,” 2016. [Online]. Available: https://ieeexplore.ieee.org/document/7858965/.

[9] D. Neves, A. Pina and C. A. Silva, “Demand response modeling: A comparison between tools,” 2015. [Online]. Available: https://www.sciencedirect.com/science/article/pii/S0306261915002342.

[10] D. Neves, A. Pina and C. A. Silva, “Assessment of the potential use of demand response in DHW systems,” 2017. [Online]. Available: https://www.sciencedirect.com/science/article/pii/S0960148117308893.

[11] D. Neves, C. A. Silva and S. Connors, “Design and implementation of hybrid renewable energy systems on micro-communities: A review on case studies,” 2014. [Online]. Available: https://www.sciencedirect.com/science/article/pii/S1364032114000021.

[12] R. Paleta, A. Pina and C. A. S. SIlva, “Polygeneration Energy Container: Designing and Testing Energy Services for Remote Developing Communities,” 2014. [Online]. Available: https://ieeexplore.ieee.org/document/6779683/.

[13] G.P.Giatrakos, T.D.Tsoutsos, P.G.Mouchtaropoulos, G.D.Naxakis and G.Stavrakakis, “Sustainable energy planning based on a stand-alone hybrid renewableenergy/hydrogen power system: Application in Karpathos island, Greece,” 2009. [Online]. Available: https://www.sciencedirect.com/science/article/pii/S0960148109002614.

[14] M. Corranda, S. J.Duncana and D. N.Mavrisb, “Incorporating Electrical Distribution Network Structure into Energy Portfolio Optimization for an Isolated Grid,” 2013. [Online]. Available: https://www.sciencedirect.com/science/article/pii/S187705091300080X.

[15] M. Soshinskaya, W. H.J.Crijns-Graus, J. v. d. Meer and J. M.Guerrero, “Application of a microgrid with renewables for a water treatment plant,” 2014. [Online]. Available: https://www.sciencedirect.com/science/article/pii/S0306261914007880.

[16] LinaMontuori, M. Alcázar-Ortega, C. Álvarez-Bel and A. Domijan, “Integration of renewable energy in microgrids coordinated with demand response resources: Economic evaluation of a biomass gasification plant by Homer Simulator,” 2014. [Online]. Available: https://www.sciencedirect.com/science/article/pii/S0306261914006576.

[17] R. H. Inman, H. T. Pedro and C. F. Coimbra, “Solar forecasting methods for renewable energy integration,” 2013. [Online]. Available: https://www-sciencedirect-com.focus.lib.kth.se/science/article/pii/S0360128513000294?via%3Dihub.

[18] D. Neves, M. C. Brito and C. A. Silva, “Impact of solar and wind forecast uncertainties on demand response of isolated microgrids,” 2015. [Online]. Available: https://www.sciencedirect.com/science/article/pii/S0960148115302755.

[19] R. Marquez and C. F. M. Coimbra, “Comparison of Clear-Sky Models for Evaluating Solar Forecasting Skill,” 2012. [Online]. Available: https://ases.conference-services.net/resources/252/2859/pdf/SOLAR2012_0575_full%20paper.pdf.

[20] A. Boilley, C. Thomas, M. Marchand, E. Wey and P. Blanc, “The Solar Forecast Similarity Method: a new method to compute solar radiation forecasts for the next day,” 2015. [Online]. Available: https://www.sciencedirect.com/science/article/pii/S1876610216303708.

[21] Capasso, Grattieri, Lamedica and Prudenzi, “A Bottom-Up Approach to Residential Load Modeling,” 1994. [Online]. Available: https://ieeexplore-ieee-org.focus.lib.kth.se/stamp/stamp.jsp?tp=&arnumber=317650.

[22] J. V. Paatero and P. D. Lund, “A model for generating househo ld electricity load profiles,” 2005. [Online]. Available: https://onlinelibrary-wiley-com.focus.lib.kth.se/doi/epdf/10.1002/er.1136.

[23] J. Widén and E. Wäckelgård, “A high-resolution stochastic model of domestic activity patterns and electricity demand,” 2009. [Online]. Available: https://www.sciencedirect.com/science/article/pii/S0306261909004930.

[24] J. Munkhammar, J. Rydén and J. Widén, “Characterizing probability density distributions for household electricity load profiles from high-resolution electricity use data,” 2014. [Online]. Available: https://www.sciencedirect.com/science/article/pii/S0306261914009167.

[25] J. A. Duffie and W. A. Beckman, “Solar Engineering of Thermal Processes,” 2013. [Online]. Available: https://onlinelibrary-wiley-com.focus.lib.kth.se/doi/book/10.1002/9781118671603.

[26] J. Duffie and W. Beckman, Solar Engineering of Thermal Processes, 2013.

[27] A. Soares, Á. Gomes and C. H. Antunes, “Categorization of residential electricity consumption as a basis for the assessment of the impacts of demand response actions,” 2013. [Online]. Available: https://www.sciencedirect.com/science/article/pii/S1364032113007181.

[28] A. Soares, A. Gomes and C. H. Antunes, “Integrated Management of Residential Energy Resources,” 2012. [Online]. Available: https://www.epj-conferences.org/articles/epjconf/pdf/2012/15/epjconf_e2c2012_05005.pdf.

[29] EDP - SENSIBLE Technical Team, 2018. [Online]. Available: N.A..

[30] International Energy Agency, “2017Portugal - Energy System OverviewENERGY,” 2016. [Online]. Available: https://www.iea.org/media/countries/portugal.pdf.

[31] C. H. Villar, D. Neves and C. A. Silva, “Solar PV self-consumption: An analysis of influencing indicators in the Portuguese Context,” 2017. [Online]. Available: https://www.sciencedirect.com/science/article/pii/S2211467X17300627.

[32] R. Luthander, J. Widén, D. Nilsson and J. Palm, “Photovoltaic self-consumption in buildings: A review,” 2014. [Online]. Available: https://www.sciencedirect.com/science/article/pii/S0306261914012859.

[33] EDP Retail, “Tarifarios 2018,” 2018. [Online]. Available: https://www.edp.pt/particulares/energia/tarifarios/.

[34] NASA, “Modern-Era Retrospective analysis for Research and Applications,” 2018. [Online]. Available: https://gmao.gsfc.nasa.gov/reanalysis/MERRA-2/.

[35] Tesla, 2018.

[36] PV Magazine, “Lithium-ion batteries below $200/kWh by 2019 will drive rapid storage uptake, finds IHS Markit,” 2017. [Online]. Available: https://www.pv-magazine.com/2017/08/03/lithium-ion-batteries-below-200kwh-by-2019-will-drive-rapid-storage-uptake-finds-ihs-markit/.

[37] Statista, “Electricity prices for households in Portugal from 2010 to 2017, semi-annually (in euro cents per kilowatt-hour),” 2018. [Online]. Available: https://www.statista.com/statistics/418111/electricity-prices-for-households-in-portugal/.

[38] A. Moro and L. Lonza, “Electricity carbon intensity in European Member States: Impacts on GHG emissions of electric vehicles,” 2017. [Online]. Available: https://www.sciencedirect.com/science/article/pii/S1361920916307933.

[39] Tomorrow, “Electricity Map,” 2018. [Online]. Available: https://www.electricitymap.org/?page=map&solar=false&remote=true&wind=false.

[40] N. Rugthaicharoencheep and S. Auchariyamet, “Technical and Economic Impacts of Distributed Generation on Distribution System,” 2012. [Online]. Available: https://pdfs.semanticscholar.org/78b0/102904f606fb89a297e97b03a5c5f30b3b8d.pdf.

[41] F. Hinz, M. Schmidt and D. Möst, “Regional distribution effects of different electricity network tariff designs with a distributed generation structure: The case of Germany,” 2017. [Online]. Available: https://www-sciencedirect-com.focus.lib.kth.se/science/article/pii/S0301421517307309.

[42] Reindl, 1988.

[43] R. Perez, P. Ineichen, R. Seals, J. Michalsky and R. Stewart, “Modeling Daylight Availability and Irradiance Components from Direct and Global Irradiance,” 1990. [Online]. Available: https://www-sciencedirect-com.focus.lib.kth.se/science/article/pii/0038092X9090055H.

Annex I: SENSIBLE Project Partners

The list of partners of the consortium is:

- Siemens AG
- ARMINES/Paris tech
- EDP NEW – Labelec/EDP Distribução
- Empower
- Green Power Technologies
- INDRA
- INESC Porto
- Mozes
- Nuremberg Institute of Technology
- University of Nottingham
- University of Seville
- Siemens S.A.
- K&S

Annex II: Data availability

Table 16: Data availability customers 1-15

	c1	c2	c3	c4	c5	c6	c7	c8	c9	c10	c11	c12	c13	c14	c15
battery input off peak	0.00%	100.00%	100.00%	96.51%	100.00%	87.27%	91.93%	100.00%	0.00%	70.42%	0.00%	99.40%	99.77%	0.00%	0.00%
battery output off peak	0.00%	100.00%	100.00%	96.57%	100.00%	87.33%	91.96%	100.00%	0.00%	70.42%	0.00%	99.46%	99.99%	0.00%	0.00%
energy from the grid off peak	99.00%	97.94%	86.88%	94.49%	95.99%	47.21%	81.21%	87.74%	53.20%	72.83%	96.52%	97.92%	94.53%	96.68%	41.75%
grid injection off peak	98.00%	99.08%	88.94%	97.23%	98.14%	48.20%	91.96%	89.37%	52.47%	75.03%	99.42%	98.68%	97.04%	98.06%	43.12%
Photovoltaic off peak night correctio	98.00%	98.90%	98.41%	100.00%	100.00%	47.03%	97.18%	100.00%	57.43%	97.10%	97.21%	98.08%	97.49%	99.31%	44.28%
water heater consumption off peak	95.38%	0.00%	29.27%	92.54%	95.07%	30.15%	0.00%	0.00%	35.73%	41.67%	98.24%	0.00%	0.00%	80.44%	34.41%
battery input peak	0.00%	0.00%	0.00%	0.00%	0.00%	33.35%	0.00%	0.00%	0.00%	0.00%	0.00%	0.00%	0.00%	0.00%	0.00%
battery output peak	0.00%	0.00%	0.00%	0.00%	0.00%	33.76%	0.00%	0.00%	0.00%	0.00%	0.00%	0.00%	0.00%	0.00%	0.00%
energy from the grid peak	0.00%	0.00%	0.00%	0.00%	0.00%	52.21%	0.00%	0.00%	38.61%	0.00%	0.00%	0.00%	0.00%	0.00%	50.33%
grid injection peak	0.00%	0.00%	0.00%	0.00%	0.00%	53.79%	0.00%	0.00%	40.33%	0.00%	0.00%	0.00%	0.00%	0.00%	52.30%
Photovoltaic peak night correction	0.00%	0.00%	0.00%	0.00%	0.00%	52.69%	0.00%	0.00%	41.35%	0.00%	0.00%	0.00%	0.00%	0.00%	53.82%
water heater consumption peak	0.00%	0.00%	0.00%	0.00%	0.00%	34.52%	0.00%	0.00%	29.41%	0.00%	0.00%	0.00%	0.00%	0.00%	46.05%

Table 17: Data availability customers 16-25

	c16	c17	c18	c19	c20	c21	c22	c23	c24	c25
battery input off peak	92.55%	0.00%	88.98%	0.00%	100.00%	0.00%	0.00%	79.38%	0.00%	77.42%
battery output off peak	92.65%	0.00%	89.26%	0.00%	100.00%	0.00%	0.00%	80.16%	0.00%	77.45%
energy from the grid off peak	87.52%	96.34%	89.14%	96.19%	38.64%	100.88%	92.30%	92.99%	80.87%	89.02%
grid injection off peak	89.27%	98.98%	91.55%	99.20%	40.37%	102.67%	94.75%	96.06%	89.28%	96.62%
Photovoltaic off peak night correctio	94.04%	97.03%	98.34%	99.46%	100.00%	101.07%	102.20%	98.01%	97.32%	99.89%
water heater consumption off peak	0.00%	80.92%	0.00%	84.91%	0.00%	70.64%	78.23%	0.00%	91.17%	0.00%
battery input peak	0.00%	0.00%	0.00%	0.00%	11.78%	0.00%	0.00%	0.00%	0.00%	0.00%
battery output peak	0.00%	0.00%	0.00%	0.00%	11.77%	0.00%	0.00%	0.00%	0.00%	0.00%
energy from the grid peak	0.00%	0.00%	0.00%	0.00%	0.00%	0.00%	0.00%	0.00%	0.00%	0.00%
grid injection peak	0.00%	0.00%	0.00%	0.00%	0.00%	0.00%	0.00%	0.00%	0.00%	0.00%
Photovoltaic peak night correction	0.00%	0.00%	0.00%	0.00%	12.56%	0.00%	0.00%	0.00%	0.00%	0.00%
water heater consumption peak	0.00%	0.00%	0.00%	0.00%	0.00%	0.00%	0.00%	0.00%	0.00%	0.00%

Annex III: Distributions for Electric Load Forecast

The Weibull probability distribution function is defined as:

Weibull PDF

$$f_W(x;\lambda,k)=\begin{cases}\frac{k}{\lambda}\left(\frac{x}{\lambda}\right)^{k-1}e^{-\left(\frac{x}{\lambda}\right)^k} & x\geq 0\\ 0 & x<0\end{cases} \tag{42}$$

Where $k>0$ is the shape parameter, and $\lambda>0$ is the scale parameter. The Weibull cumulative distribution function is:

Weibull CDF

$$F_W(x;\lambda,k)=\begin{cases}1-e^{-\left(\frac{x}{\lambda}\right)^k} & x\geq 0\\ 0 & x<0\end{cases} \tag{43}$$

When $k=1$, the Weibull distribution corresponds to the exponential distribution, while when $k=2$ it is equivalent to the Rayleigh distribution. The mean value is:

Weibull mean

$$\mu=\lambda\Gamma\left(1-\frac{1}{k}\right) \tag{44}$$

The variance is:

Weibull variance

$$\sigma^2=\lambda^2\Gamma\left(1+\frac{2}{k}\right)-\mu^2 \tag{45}$$

Where $\Gamma(x)$is the Gamma function. The Log-Normal PDF of the random variable L is defined as:

Log-Normal PDF

$$f_L(x;\mu,\sigma)=\frac{1}{x\sigma\sqrt{2\pi}}e^{-\frac{(\ln x-\mu)^2}{2\sigma^2}}\quad x>0 \tag{46}$$

Where μ is the mean and σ^2 is the variance. The Log-Normal CDF is:

Log-Normal CDF

$$F_L(x;\mu,\sigma)=\frac{1}{2}\left[1+\operatorname{erf}\left(\frac{\ln(x)-\mu}{\sigma\sqrt{2}}\right)\right] \tag{47}$$

Where $\operatorname{erf}(x)$ is the error-function defined as:

Eq.

$$\operatorname{erf}(x)=\frac{2}{\sqrt{\pi}}\int_0^x e^{-t^2}\,dt \tag{48}$$

Annex IV: Electric Load Modelling

Clustering by hour, weekday and month

The first criteria have selected for clustering the electric load data aims to create distributions of probability for each timestep, based on the observations from the data, sorted:

- By month: considers the seasonal variability;
- By weekdays or weekends: considers the different habits of a family, if the working days are from Monday to Friday;
- By hour: allows to generate a electric load profile for each day, with a fixed timestep. The load is considered constant within the timestep.

A schematic overview is presented in Figure 54, where the unit of the model is identified.

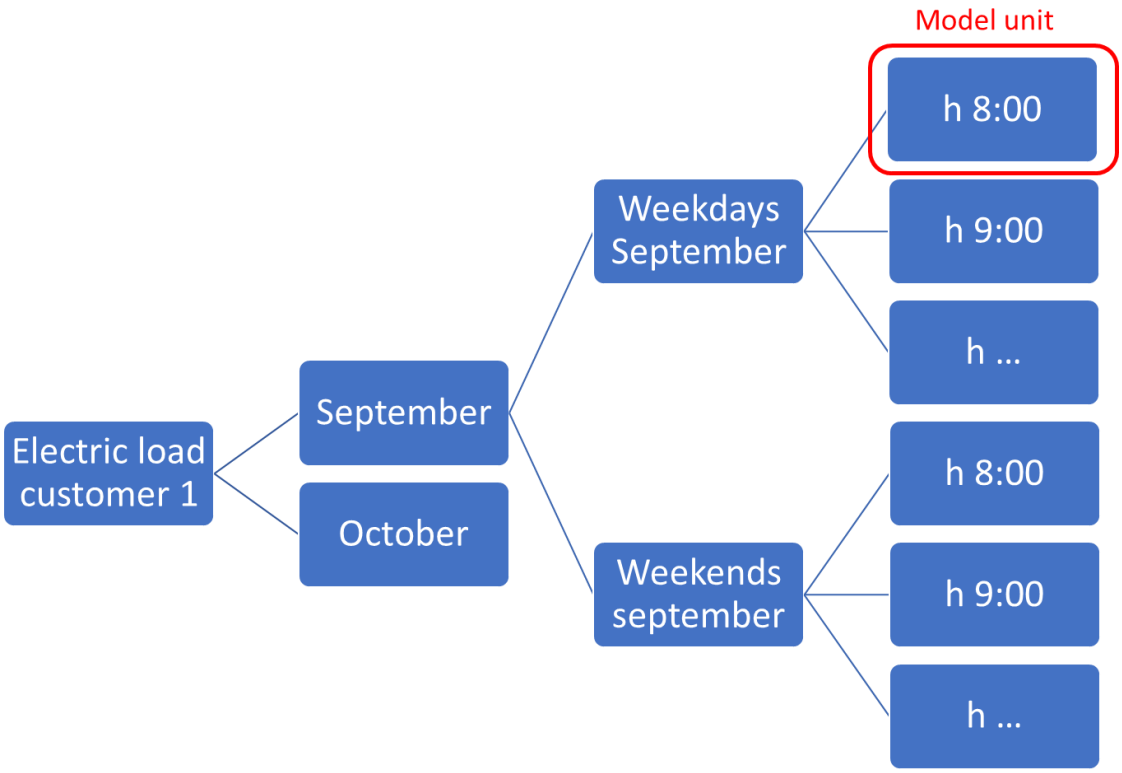

Figure 54: Data clustering by month, by weekday and by hour

Having the data sorted according to this scheme, for each distribution it is possible to identify outliers with the equation xxx and to remove them from the dataset.

The resulting model will be a concatenation of distributions, representative of each model unit, that can be used to:

- Generate a load curve with a Montecarlo method, to make predictions for the electricity consumption;
- Fill the gaps in the dataset using average values, an example is shown in Figure 55.

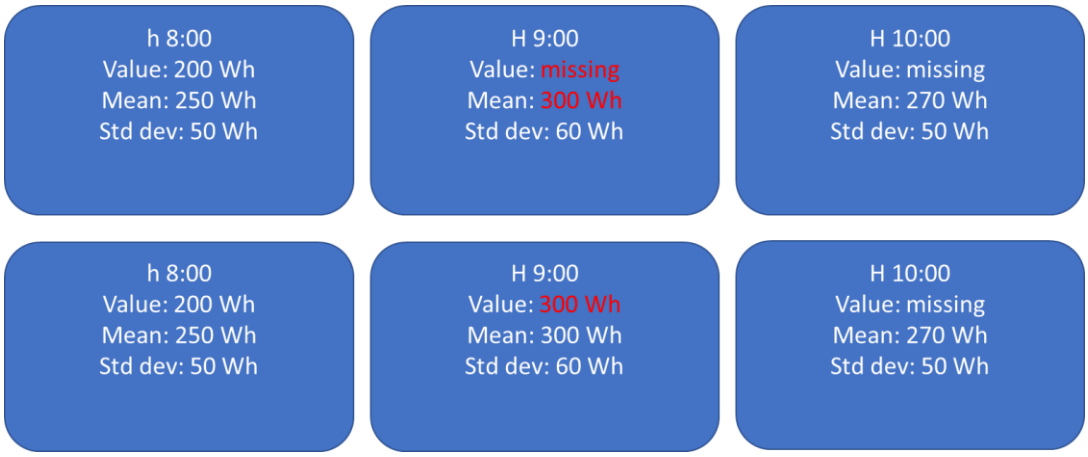

Figure 55: Filling data gaps

Clustering by daily consumption, weekday and month

This clustering strategy is similar to the previous one, divided by month and weekdays. The difference lies in the model unit, which is not the single hour but the daily consumption.

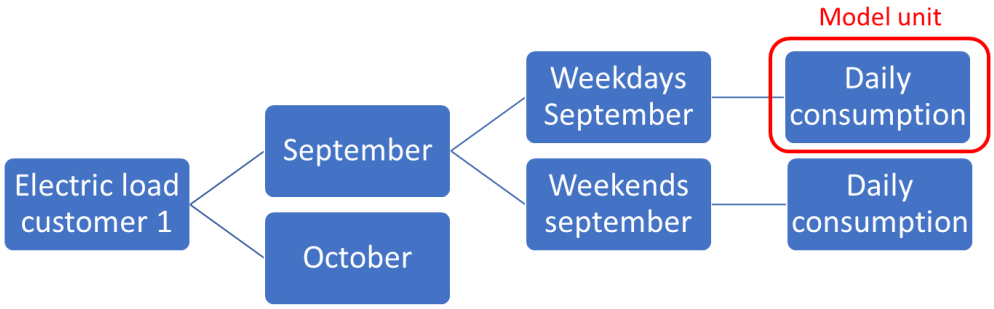

Figure 56: Data clustering by month, by weekday and daily consumption

It is possible to identify distributions of the daily consumptions for each period of the year, calculating mean and standard deviation. Then the model can be built by selecting for each period a "typical day", the closest to the mean value: this day will be repeated for the whole period represented, returning a model with two typical days per month, 24 in a year. Additionally, day by day variability can be included taking into account the standard deviation of the period considered, starting from the model day selected.

Annex V: Solar angles

A_i is the anisotropy index, function of the transmittance of beam radiation of the atmosphere. It determines the portion of the horizontal diffuse radiation that can be considered forward scattered, with the same incidence angle of beam radiation.

$$A_i = \frac{G_b}{G_0}$$

When conditions are of clear sky, A_i is high and most of the diffuse radiation is forward scattered. In overcast conditions, when there is no beam radiation, A_i is zero and all the diffuse radiation is isotropic.

Eq.

$$B = (n-1)\frac{360}{365} \quad (49)$$

Where n is the day of the year according to the Gregorian Calendar.

The clearness index can be calculated using the measurement of the global horizontal irradiance of the pyranometer, and the extra-terrestrial irradiance on a horizontal surface:

Eq.

$$k_T = \frac{G}{G_0} \quad (50)$$

Once the clearness index has been calculated as presented above, the next step is to correlate Gd/G, the fraction of the irradiance on a horizontal plane which is diffuse, with kT, the hourly clearness index. This is made based on correlations presented in the literature [42]. Figure 57 shows the correlations for the mean irradiation, valid also for the irradiance.

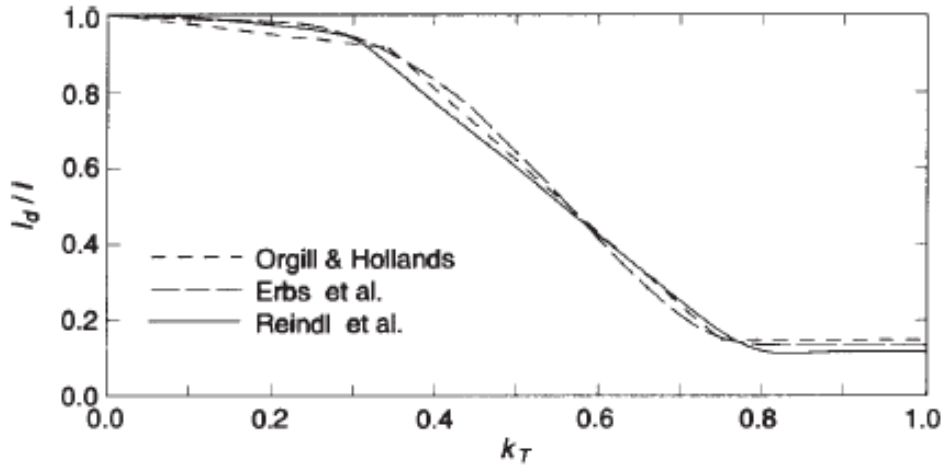

Figure 57: The ratio Id/I as function of hourly clearness index kT showing the Orgill and Hollands (1977), Erbs et al. (1982), and Reindl et al. (1990a) correlations.

The equations used for the sake of the project were the following:

$$Eq. \quad \frac{G_d}{G} = \begin{cases} 1 - 0.09k_t \; for \; k_t \leq 0.22 \\ 0.9511 - 01604k_t + 4.388{k_t}^2 - 16.638{k_t}^3 + 12.336{k_t}^4 \; for 0.22 < k_t \leq 0.8 \\ 0.165 \; for \; k_t > 0.8 \end{cases} \quad (51)$$

The beam fraction (Gb/G) is the complement of the diffuse fraction, so it is calculated as 1 - Gd/G. Most of the irradiance is diffuse during morning, but the beam raises quickly reaching the peak around noon.